Micro-Bubbles Enhance Photon Utilization Efficiency in Ultraviolet-Based Advanced Oxidation Processes

by

Hafiz Hamza

A Thesis Submitted to the Faculty of Graduate and Postdoctoral Studies of

The University of Manitoba

in partial fulfillment of the requirements for the degree of

Master of Science

Department of Civil Engineering

University of Manitoba

Winnipeg

December 2025

Acknowledgement

I would like to express my sincere gratitude to my supervisor, Dr. Qiuyan Yuan, for her guidance, encouragement, and continuous support throughout this research. Her insight, patience, and constructive feedback were invaluable in shaping this work and in helping me grow as a researcher.

I am also very thankful to my co-supervisor, Dr. Chengjin Wang for his thoughtful suggestions, technical advice, and support during different stages of this study. His expertise and perspective greatly contributed to the development and refinement of this research.

I would like to acknowledge the members of my thesis committee Dr. Nazim Cicek and Dr. Beata Gorczyca for their time, valuable comments, and constructive feedback, which helped strengthen the quality and clarity of this thesis.

I am deeply grateful to my parents for their unconditional love, sacrifices, and constant encouragement. Their prayers, patience, and belief in me have been my greatest source of strength throughout this journey. I would also like to thank my uncle, auntie and my brother for their support, understanding, and motivation during my studies.

I would like to extend my appreciation to my colleagues and lab mates for their help, discussions, and collaborative spirit, which made the research process both productive and enjoyable. Their support and friendship created a positive and motivating research environment.

Finally, I would like to thank my friends for their encouragement, understanding, and support throughout my academic journey. Their presence and positivity made this experience more meaningful.

ABSTRACT

Micropollutants are important issues in water treatment because some of them pose health risks to humans and the environment. Ultraviolet-based advanced oxidation processes (AOPs) have emerged to be effective in micropollutant control, which rely on UV photons to split oxidants into radical species that can destroy micropollutants. However, the photon utilization efficiency in most UV-based advanced oxidation processes (AOPs) is usually low, and the fundamental reason is that the UV photons travel too short a path length in the water before they hit and be absorbed by the reactor walls and other accessories (i.e., be wasted). To address this issue, this study integrated microbubbles into the system to "trap" photons in the water. The surfaces of numerous microbubbles scatter or reflect photons, changing the photons' pathways from straight to torturous. This will keep the photons in the water long enough to interact with oxidants and less likely to reach the walls, resulting in performance enhancement.

This study is designed to compare two widely used AOPs, UV/H_2O_2 and UV/chlorine, in micropollutant control at bench scale, with and without microbubbles. Nitrobenzene, benzoic acid, and caffeine are selected as representative micropollutants. The impact of microbubbles on AOP performance is evaluated under different conditions by monitoring the kinetics of oxidant (i.e., H_2O_2 or chlorine) and micropollutant decay and are quantified using the enhancement ratio $k_{air}/k_{no\text{-}air}$. The different test conditions are achieved by varying oxidant doses, reactor sizes (short vs long path lengths), water matrices (low transmittance vs high transmittance), and lamp types (low pressure and medium pressure). Microbubbles were generated using a CARMIN diffuser, producing stable bubbles predominantly in the 10 –100 μm range.

Results showed that aeration consistently enhanced oxidant decay and micropollutant removal, confirming that microbubbles improve photon availability by scattering and reflecting UV light within the reactor. The magnitude of enhancement depended on oxidant dose, bubble concentration, reactor geometry, and lamp type. Medium-pressure UV lamps exhibited the strongest response to aeration, given their broader emission spectrum and greater baseline photon losses. A distinct optimal bubble concentration was identified; too many bubbles reduced UV penetration, while too few provided minimal scattering benefit.

Overall, the findings demonstrate that microbubble-enhanced UV-AOPs offer a promising pathway to improve treatment performance, reduce photon losses, and optimize energy use in water treatment systems. The study provides experimental evidence and practical insights that can guide future reactor design, optimization of bubble parameters, and scale-up of aeration-assisted UV technologies.

Table of Contents

List of Tables

List of Figures

CHAPTER 1: INTRODUCTION

1.1 Background

Water is an essential resource for life, economic development, and environmental sustainability. However, with the increased rate of urbanization, industrialization and rise in agriculture practices, water pollution with various hazards has increased across the world (Lin et al., 2022). Of these contaminants, Micropollutants are important issues in water treatment because some of them pose health risks to humans and the environment. They are chemicals present in very small concentrations that are likely to be highly damaging since they do not leave the water cycle and can produce detrimental impacts on human health and the ecosystem (El Hammoudani et al., 2024). Ultraviolet-based advanced oxidation processes (AOPs) have emerged to be effective in micropollutant control, which rely on UV photons to split oxidants into radical species that can destroy micropollutants. However, the photon utilization efficiency in most UV-based advanced oxidation processes (AOPs) is usually low, and the fundamental reason is that the UV photons travel too short a path length in the water before they hit and be absorbed by the reactor walls and other accessories (i.e., be wasted). To address this issue, this study integrated microbubbles into the system to "trap" photons in the water. The surfaces of numerous microbubbles scatter and reflect photons, changing the photons' pathways from straight to torturous. This will keep the photons in the water long enough to interact with oxidants and less likely to reach the walls, resulting in performance enhancement. This study addresses this issue by incorporating microbubbles into UV-AOP systems. Microbubbles scatter and reflect photons, altering their path from straight to more tortuous, which prolongs their residence time in the reactor, thereby enhancing the interaction with oxidants. The effect of microbubbles on AOP performance was evaluated using two common UV-AOPs, UV/H_2O_2

and UV/chlorine, at bench scale, with micropollutants such as caffeine, benzoic acid, and nitrobenzene serving as test compounds. The study investigated the influence of different oxidant doses, reactor sizes, water matrices, and UV lamp types (low pressure and medium pressure). For each test condition, the optimal microbubble concentration for enhancing photon utilization identified experimentally. This chapter presents research problem and objectives, as well as the structure of the thesis.

1.2 Research Problem Statement and Objectives

The inefficiencies in traditional UV reactors, primarily due to photon absorption by reactor walls and poor light path management, present a significant hurdle in the effective treatment of micropollutants. Although there have been some degrees of success in the application of traditional schemes like incorporating reflectors, they come with complications like maintenance, fouling problems, and degradations in their performance over a period.

1.2.1 Research Problem Statement

This research seeks to address the following problems:

“How can the integration of aeration into UV reactors enhance photon utilization and improve the degradation efficiency of micropollutants in water treatment?”

To address this problem, the study will focus on evaluating the effect of air bubble injection on the decay rates of oxidants and micropollutants within UV-based advanced oxidation processes. Previous studies have demonstrated that despite even a well-designed reactor having very high conversion efficiency, there are immense UV photon losses due to the reactor system design; nevertheless, the role of aeration in mitigating these losses has not been paid much attention.

1.2.2 Research Objectives

The specific objectives of this study are as follows:

1. Evaluate the Effect of Aeration on Oxidant Decay Rates: To compare the decay rates of oxidants (such as chlorine and hydrogen peroxide) in UV reactors under aerated and non-aerated conditions.

2. Optimize Bubble Size and Concentration: To investigate the influence of bubble size and concentration on enhancing photon utilization rate.

3. To investigate the effect of flow rate on bubble generation and distribution in a UV-AOP reactor, and to determine the optimum flow rate that maximizes both oxidant decay and micropollutant degradation.
4. Determine the Impact of Aeration on Micropollutant Degradation: To monitor and quantify the degradation rate of representative micropollutants caffeine, benzoic acid, and nitrobenzene using UV-based AOPs.
5. Develop Recommendations for Applications: Based on the experimental findings, to provide practical recommendations for the integration of aeration-assisted UV AOPs in water treatment systems.

   This study is designed to address the fundamental principles of the aeration-assisted approach. It seeks to enhance understanding of the interactions among UV light, oxidants, and air bubbles within advanced oxidation processes (AOPs), with the broader aim of contributing to the development and improvement of water treatment technologies.

1.3 Thesis Structure Overview

This thesis is structured into five chapters to systematically address the research problem, review the relevant literature, present experimental findings, and discuss the implications of the study.

1.3.1 Chapter 2: Literature Review

In this chapter a critical review of the literature on micropollutants, their sources as well as the effect they have on human beings, and the environment will be discussed. It will describe and analyze the principles of advanced oxidation processes particularly those which use UV light and will focus on the effects of photons on reactor performances. Also, it will discuss previous practices of improving the reactor performance including reflecting material and evaluate the limitations of other water treatment processes. This section will discuss the methods for the generation and techniques for the quantification of bubbles as well as gaps of knowledge as the basis for the present research.

1.3.2 Chapter 3: Methodology, Results and Discussion

This chapter outlines the experimental procedures used to investigate the effects of microbubble aeration on the performance of UV-based Advanced Oxidation Processes. It details the design and operation of the UV reactors, the method of microbubble generation and characterization, and the analytical techniques used to quantify both oxidant decay (hydrogen peroxide and free chlorine) and micropollutant degradation (caffeine, benzoic acid, and nitrobenzene). The chapter then presents the full set of results, beginning with microbubble size distribution, followed by oxidant decay kinetics under aerated and non-aerated conditions, and concluding with the degradation behavior of the selected micropollutants. A comprehensive discussion interprets these findings, linking them to photon utilization

efficiency, bubble-induced light scattering, reactor geometry, and oxidant chemistry. Together, these analyses provide a deeper understanding of how microbubble integration enhances the overall treatment performance of UV-AOP systems.

CHAPTER 2: LITERATURE REVIEW

This chapter provides a comprehensive review of the existing literature on micropollutants in the aquatic environment and the use of advanced oxidation processes (AOPs) for their degradation. It also discusses the behavior of photons within UV reactors and the use of reflectors to improve light distribution and treatment efficiency. By summarizing previous studies and highlighting different research perspectives, this chapter identifies the key limitations in current approaches and outlines how the present work aims to address these gaps, contributing to a better understanding and optimization of UV-based AOP systems.

2.1 Global Water Quality Challenges

Water quality has emerged as a critical global challenge in recent decades. Increased industrialization, rate of population growth, and increased rate of farming practices are some of the causes of water pollution on a worldwide basis (Shannon et al., 2008). Whereas earlier attention was paid to nutrient, heavy metals, and pathogen content, The emergence of micropollutants in the environment has increasingly become a significant global issue. The presence of these pollutants, even in very low concentrations, represents a serious risk to both ecosystems and human health, owing to their persistence, ability to accumulate in living organisms, and potential to disturb fragile ecological systems (Sharma et al., 2024). This includes a wide range of compounds such as active pharmaceutical residues, personal care products, steroid hormones, antibiotics, cosmetics, flame retardants, food additives, pesticides, endocrine disruptors, and industrial chemicals (Morin-Crini et al., 2022). Many micropollutants find their way into the environment via industrial effluents, wastewater treatment plants, agricultural runoff, and atmospheric deposition (Ahmad et al., 2019). Water bodies are found to have micropollutants present in very low concentrations (µg/L to ng/L) (Ajala et al., 2022). The identification and analysis of these micropollutants present a challenge

for traditional wastewater treatment methods to effectively eliminate them (Y. Zhang et al., 2022). Consequently, releasing wastewater that contains these enduring micropollutants may present a considerable risk to human health and the natural environment (Narwal et al., 2023). The presence of these pollutants can disrupt the endocrine systems of aquatic organisms, leading to complications in reproduction and development. These substances can accumulate in the food chain, potentially impacting humans who eat contaminated aquatic organisms. The persistence and low concentration of these micropollutants pose significant risks because even minute amounts can elicit biological responses. Several research highlighted that they could exert such impacts on aquatic life; they also pose threats to human health via water supplies (Petrie et al., 2015). For example, some of the endocrine disruptors affect the reproductive system of fish and wildlife and similar effects could be expected in human beings because of chronic exposure (Marlatt et al., 2022). They also cause the more complex challenge of antibiotic resistant micropollutants in water (Cizmas et al., 2015).

2.1.1 Classification of Micropollutants

Micropollutants primarily consist of pharmaceuticals and personal care products (PPCPs), pesticides, polycyclic aromatic hydrocarbons (PAHs), pharmaceutical active compounds (PACs), polychlorinated biphenyls (PCBs), endocrine disruptors, volatile organic compounds, and various industrial chemicals (Gupta et al., 2022; Postigo et al., 2021). PPCPs enter the environment via wastewater discharge, sewage treatment facilities, human excretion, expired medications, and livestock farming. Their presence has been detected in surface water, groundwater, and drinking water resources (K'oreje et al., 2018; Kucuk et al., 2021). For example, sulfamethoxazole, an antimicrobial frequently employed to address infections in humans and animals, is not fully metabolized, and its metabolites (N-acetyl-sulfamethoxazole) are released through excretion in urine and feces into wastewater treatment facilities,

agricultural runoff, and farmland when farmyard manure is applied as fertilizer (Grenni et al., 2019). Micropollutants originating from the pharmaceutical industry present considerable environmental issues, as they demonstrate low biodegradability, exert toxicity on aquatic ecosystems even at trace levels, and may impact on human health when ingested via drinking water (Varsha et al., 2022). Table 1 shows different types of micropollutants and their environmental impact

Table 1. Different types of micropollutants and their environmental impact (Sharma et al., 2024).

Micropollutants	Applications	Environmental Impact	Concentration
Petroleum hydrocarbon	Lubricants and greases (Polycyclic aromatic hydrocarbon)	Carcinogenic, mutagenic, and teratogenic effects in humans. Cause accumulation of persistent compounds in the environment.	52-997 1678–6748 mg/kg (wasteland) 1189–2239 mg/kg (farmland) 1089–2239 mg/kg (Wetland)
Ethylbenzene	Production of styrene	GI tract irritation in humans Chronic toxicity on fish embryos	16160 ng/L
Dichloromethane	Aerosol propellant (Organochlorine compound)	Exposure to high concentration may cause irritation to lungs, Damage to brain and liver	3010 ng/L
Caffeine	Stimulant	Disturbs sleeping patterns in humans. Exerts developmental toxicity in fish	7 ng/L

2.1.2 Sources of Micropollutants

Micropollutants can originate from multiple sources and pathways. Key sources include Municipal wastewater, industrial discharges, pharmaceuticals and agricultural runoff.

Most of the micropollutants reach water bodies through the discharge of the effluent from wastewater treatment plants. Housings are often populated with pharmaceuticals, personal care products and other chemicals that normal treatment plant can seldom treat (Verlicchi & Ghirardini, 2019). These treatment plants are generally designed to remove conventional pollutants such as organic matter and pathogens, but they struggle to effectively eliminate micropollutants due to their low concentrations and chemical complexity. As a result, many micropollutants pass through treatment processes and are discharged into receiving water bodies, contributing to their persistent presence in the environment (Pistocchi et al., 2022). Industries such as chemical manufacturing, mining, and electronics produce a variety of persistent organic pollutants. These chemicals are mostly discharged directly into nearby water sources or admitted through leachate from polluted areas (Ankit et al., 2021). Some of these contaminants enter the environment directly via wastewater outfalls, while others leach into groundwater or surface waters from contaminated soils and waste disposal sites. The complexity and variability of industrial effluents pose challenges for conventional treatment, often resulting in the accumulation of recalcitrant compounds in aquatic ecosystems over time (Nishmitha et al., 2025). Veterinary and human pharmaceuticals have been identified in aquatic environments mainly because of discharge and excretion. These compounds retain their bioactivity at subparts per billion levels interfering with endocrine system of affected organisms (Kayode-Afolayan et al., 2022). Even at extremely low concentrations—often in the subparts-per-billion range pharmaceuticals maintain their bioactivity and can interfere with the endocrine systems of aquatic organisms. This interference may lead to disruptions in reproduction and development, raising concerns about long-term ecological and human health impacts (Samal et al., 2022).

The use of pesticides, fertilizers, and veterinary drugs in agriculture results in the runoff of these chemicals into streams and groundwater. Pesticides are particularly toxic to non-target

species, causing acute toxicity as well as chronic effects that impair ecosystem functions. Additionally, some pesticides and their degradation products are persistent in the environment, leading to bioaccumulation and long-lasting ecological consequences. Fertilizer runoff can also contribute to eutrophication, which may influence the fate of micropollutants and further impact aquatic health (Stehle & Schulz, 2015).

2.1.3 Occurrence and Distribution

The occurrence and distribution of micropollutants in the water environment have been widely documented in recent decades. Such contaminants are prevalent in surface water, ground water as well as wastewater (Jiang et al., 2024). Among them, surface water has been recognized as one of the major sources of micropollutants as effluents generated from untreated or partially treated wastewater discharge, agricultural wastewater, and industrial effluents (Singh et al., 2023). Monitoring surveys of micropollutants were conducted in the rivers, lakes and reservoirs across most European, North American and Asian countries wherein concentrations ranged from the ng/L to µg/L levels in most of the cases as stated by Dar et al. (2025) and Kaur et al., (2020). Groundwater contamination is another emerging concern, as infiltration from surface water and leachate from landfills contribute to the presence of micropollutants in aquifers (Pradhan et al., 2023). Many papers have documented that concentrations of contaminants appear to be lower in groundwater than in surface water; however, the natural biological degradation processes are very ineffective in removing these contaminants from both groundwater due to limited oxygen and microbial activity and surface water, where dilution and variable photolysis limit persistence (Abanyie et al., 2023; Romantschuk et al., 2023; Luo et al., 2014)Micropollutants are frequently detected in both the influent and the effluent, reflecting the ineffectiveness of the generally used WWTPs in eradicating these substances (Belete et al., 2023).

The spatial and temporal distribution of these contaminants has been mapped by several global monitoring programs. For example, the research cases of European regions have revealed that micropollutant contamination is high in urbanized-industrialized areas (Innocenzi et al., 2020). The various comparative mapping analyses may employ geographic information systems (GIS) to associate contamination rate with population, industrial production, and efficiency of the wastewater treatment plants (Awawdeh et al., 2023). Trends in micropollutants also present variation of levels in the years; such variations are due to changes in industries, improved wastewater treatment, regulations, and shift in use of pharmaceutical and personal care products by the consumers (Jiang et al., 2024).

2.1.4 Health and Environmental Impacts

The effects of micropollutants are diverse and can lead to significant health and adverse environmental impacts. High concentrations of micropollutants have been proved to cause health issues in humans; however, recent studies have also verified that even in small amount, these particles can lead to various diseases associated with hormonal imbalances, reproductive disorders, and increased occurrences of cancers. (El Hammoudani et al., 2024). Further, the evolution of antibiotic-resistant bacteria that can be partly attributed to low-concentration chronic exposure to antibiotics through treated sewage water constitutes to be a matter of concern in public health (Martinez, 2009). Polychlorinated biphenyls (PCBs) and polyfluoroalkyl substances (PFAS) are examples of persistent chemicals that have been linked to immune system problems, liver toxicity, and neurodevelopmental issues, especially in children whose growing bodies make them more sensitive to chemicals (Post et al., 2012; Carpenter, 2006). In terms of the environment, micropollutants have been linked to endocrine disruption in aquatic species, which changes how they reproduce and makes their populations less likely to survive (Mustafa et al., 2024). Dioxin and furan are two examples of

micropollutants that are known to be persistent and bio accumulative. They tend to build up in the tissues of living things, and their concentrations get higher as you move up the food chain (Rogowska et al., 2019). Wastewater releases that contain pharmaceuticals, antibiotics, and personal care items have been shown to change the behavior, reproduction, and survival of aquatic creatures including fish, amphibians, and invertebrates (Kümmerer, 2009). The accumulation of these pollutants can harm the habitat, which can modify the biological characteristics of aquatic ecosystems. Recent studies throughout the world have shown these effects, which shows that we need more ways to address these toxins to stop them from spreading (Nimma et al., 2025).

2.2 Traditional Water Treatment Methods

Traditional water treatment methods have been designed to tackle conventional pollutants such as suspended solids, organic matter, and pathogenic microorganisms. Some of the widely used mechanisms include Coagulation. These are processes that cause the colloidal particles to group together into a bigger floc that can easily be separated through sedimentation or filtration. Sedimentation after coagulation, water is left to stand still so that heavier particles can specifically be settled through the force of gravity. Filtration for instance, by sand filtration or other membrane techniques, this process involves separation of contaminants. Chlorination final one is the chlorination process where chlorine is used for disinfecting the water by eliminating pathogenic microorganisms (Castro-Jiménez et al., 2022). The conventional treatments can be categorized into three main groups: physical, chemical, and biological treatments. The advantages and disadvantages of these traditional treatments are summarized in Table 2.

Table 2. Water treatment techniques with advantages and disadvantages (Cuerda-Correa et al., 2020).

	Physical or Physicochemical Treatment	**Biological Treatment**	**Chemical Treatment**
Kind of pollutant	Industrial (organic, inorganic, metals)	Industrial and domestic (low concentrations of organic and some inorganic)	Industrial (organic, inorganic, metals)
Methods	Filtration Adsorption Air floatation Extraction Flocculation Sedimentation	Anaerobic Aerobics Activated muds	Thermal oxidation (combustion) Chemical oxidation Ion exchange Chemical precipitation
Advantages	Low cost of capital Relatively safe Easy to operate	Easy maintenance Relatively safe elimination of the dissolved contaminants Easy to operate	High degree of treatment Elimination of the dissolved contaminants
Disadvantages	Volatile emissions High energetic cost Complex maintenance	Volatile emissions Require elimination of residual muds Susceptible to toxins or antibiotics	High costs of capital and operation. Difficult operation

2.2.1 Non-UV Based Methods

- Ozonation
- Membrane Filtration
- Biological Treatment

- Adsorption Technique

Conventional treatment technologies such as ozonation, membrane filtration, biological treatment, and adsorption techniques have been extensively applied for water and wastewater purification. However, these methods often show limited efficiency in eliminating emerging organic contaminants (EOCs), such as pharmaceuticals (e.g., caffeine, diclofenac), personal care products (e.g., triclosan, parabens), pesticides, and industrial chemicals (e.g., bisphenol A, nonylphenol). These compounds are characterized by their chemical stability and resistance to biodegradation, which allows them to persist through traditional treatment systems. For instance, ozonation and absorption primarily transfer pollutants from water to another phase, such as sludge or activated carbon, without achieving full mineralization (Pulicharla et al., 2020) (Sturm et al., 2022). Membrane filtration, while effective for separation, often suffers from membrane fouling and high operational costs (Abdel-Fatah, 2018). Similarly, biological processes are limited by the poor biodegradability of many EOCs, resulting in incomplete removal (Kumari and Kumar, 2023). In contrast, Advanced Oxidation Processes (AOPs) particularly UV-based systems generate highly reactive hydroxyl radicals that can oxidize and mineralize complex organic molecules into harmless end products such as CO_2 and H_2O. Therefore, AOPs offer a more robust and sustainable solution for the degradation of persistent micropollutants, overcoming the key limitations of conventional treatment approaches.

2.3 Overview of Advanced Oxidation Processes (AOPs)

2.3.1 Definition and Mechanism of AOPs

Advanced oxidation processes (AOPs) are a collection of chemical treatment procedures designed to remove organic and inorganic contaminants from water by generating reactive

species, primarily hydroxyl radical (•OH). These radicals are highly reactive due to the point that they have a high oxidative power; thus, they reduce complex and persistent molecules into less complicated molecules which are often harmless (Pera-Titus et al., 2004). The idea behind using AOPs is the generation of these radicals on the site by chemical/ photochemical means and the fact that they non selectively react with most common pollutants like antibiotics, pharmaceutical, and volatile and semi-volatile organic compounds (Khader et al., 2024). The efficiency of AOPs is largely dependent on the generation rate and availability of these reactive species. In UV based AOPs, the reaction usually starts with the absorption of UV photons by an oxidant which may be hydrogen peroxide or chlorine. This results in the formation of hydroxyl radicals that in turn react with the pollutant molecules and produce various by products. For instance, the UV/H_2O_2 reaction often makes aldehydes and alcohols, as well as low-molecular-weight organic acids like formic and acetic acid. But the UV/Cl_2 process may lead to the generation of disinfection by-products, such as trihalomethanes (like chloroform) and haloacetic acids, as well as inorganic compounds like chlorate and perchlorate. Different factors, including different kinds of pollutants, the water matrix, and the conditions under which the treatment is done, affect the properties and amounts of these byproducts. This emphasizes the necessity for an optimized treatment design (Kumari & Kumar, 2023). Hydroxyl radicals are ideal among powerful oxidants since they fulfill certain criteria: (Ameta & Ameta, 2018)

- Rapid reaction rates, usually in the order of 10^9 M^{-1} s^{-1} (Hoigné, 1998; Buxton et al., 1988)
- They do not produce extra waste.
- They are non-toxic and possess a short lifespan.
- They do not cause corrosion to equipment components (Pignatello et al., 2006)

Simple assembly methods are typically used for the generation of hydroxyl radicals. Based on these considerations, AOPs are environmentally compatible technologies, and competitive processes from an economic perspective are being developed. The Standard reduction potential in aqueous medium for the most frequently utilized oxidizing agents is presented in Table 3. The effectiveness of the AOPs is based upon the performance of the OH radical, recognized as the second species with greater oxidizing capability following fluorine. (Hoigné, 1998)

Table 3. Standard reduction potentials in aqueous medium for the most frequently utilized oxidizing agents(Cuerda-Correa et al., 2020).

Oxidizer	Reduction Reaction	E°/V
Fluorine	$F_2(g) + 2H^+ + 2e^- \rightarrow 2HF$ $F_2(g) + 2e^- \rightarrow 2F^-$	3.05
Hydroxyl radical	$OH + H^+ + e^- \rightarrow H_2O$	2.80
Sulfate radical anion	$SO_4^- + e^- \rightarrow SO_4^{2-}$	2.60
Ferrate	$FeO_4^{2-} + 8H^+ + 3e^- \rightarrow Fe^{3+} + 4H_2O$	2.20
Ozone	$O_3(g) + 2H^+ + 2e^- \rightarrow O_2(g) + H_2O$	2.08
Peroxydisulfate	$S_2O_8^{2-} + 2e^- \rightarrow 2SO_4^{2-}$	2.01
Hydrogen peroxide	$H_2O_2 + 2H^+ + 2e^- \rightarrow 2H_2O$	1.76
Permanganate [a]	$MnO_4^- + 4H^+ + 3e^- \rightarrow MnO_2(s) + 2H_2O$	1.67
Hydroperoxyl radical [a]	$HO_2 + 3H^+ + 3e^- \rightarrow 2H_2O$	1.65
Permanganate [b]	$MnO_4^- + 8H^+ + 5e^- \rightarrow Mn2^+ + 4H_2O$	1.51
Hydroperoxyl radical [b]	$HO2 + H^+ + e^- \rightarrow H_2O_2$	1.44
Dichromate	$Cr2O7^{2-} + 14H^+ + 6e^- \rightarrow 2Cr^{3+} + 7H_2O$	1.36
Chlorine	$Cl_2(g) + 2e^- \rightarrow 2Cl^-$	1.36
Manganese dioxide	$MnO_2 + 4H^+ + 2e^- \rightarrow Mn^{2+} + 2H_2O$	1.23
Oxygen	$O_2(g) + 4H^+ + 4e^- \rightarrow 2H_2O$	1.23
Bromine	$Br_2(l) + 2e^- \rightarrow 2Br^-$	1.07

[a]) Circumneutral or weakly acidic medium; [b] Strongly acidic medium

2.3.2 Types of UV-Based AOPs

UV-based systems are among the most used AOPs because they can rapidly generate reactive radicals, such as hydroxyl radical (•OH), which are highly effective in degrading pollutants

(Pignatello et al., 2006; Miklos et al., 2018). These systems typically produce fewer undesirable or toxic secondary by-products compared to other chemical treatments like chlorination, which can form harmful compounds such as trihalomethanes (THMs) or haloacetic acids (HAAs) (Richardson et al., 2007; von Gunten, 2003). Common UV-driven processes include:

UV/H_2O_2 System

The UV/H_2O_2 process is one of the most widely studied and implemented photochemical AOPs(Pignatello et al., 2006; Miklos et al., 2018). Upon irradiation with UV-C light (typically at 254 nm), hydrogen peroxide (H_2O_2) undergoes homolytic cleavage, generating two hydroxyl radicals:

$$H_2O2 + h\nu \rightarrow 2 \cdot OH \quad (1)$$

The quantum yield of this process is exceptionally high, producing a maximum of two hydroxyl radicals as absorbed, and remains constant regardless of the applied wavelength.

$$H_2O_2 + OH \rightarrow HO_2\cdot + H_2O \quad (2)$$

$$H_2O_2 + HO_2^{\bullet} \rightarrow OH + O_2 + H_2O \quad (3)$$

$$2\ HO_2^{\bullet} \rightarrow H2O_2 + O_2 \quad (4)$$

$$OH + HO_2\cdot \rightarrow H_2O_2 + O_2 \quad (5)$$

From Reactions (2) – (5), while the photolytic cleavage of hydrogen peroxide leads to the generation of ·OH radicals (Reaction (1), the presence of higher concentrations of H_2O_2 could potentially scavenge these hydroxyl radicals Rection (2), thereby impeding the efficiency of the oxidation process. Therefore, it is essential to carefully adjust the initial concentration of H_2O_2 to optimize the effectiveness of the removal process(Cédat et al., 2016). Upon the formation of the highly reactive ·OH radicals, they engage with the organic compound through various mechanisms: the abstraction of a hydrogen atom, addition to C=C double bonds, or

electron transfer, based upon nature and functional groups of the molecule. Hydroxyl radicals formed in this manner possess a redox potential of approximately 2.8 V, enabling them to degrade into a wide range of organic pollutants, including pharmaceuticals, endocrine-disrupting compounds, and pesticides (Chen et al., 2021).

UV/Chlorine System

Chlorine-based disinfection technologies are used in most drinking water treatment systems. These technologies add free chlorine as chlorine gas (Cl2) or sodium hypochlorite (NaOCl) to make hypochlorous acid (HOCl) and hypochlorite ions (OCl-). Conventional treatment processes in wastewater treatment facilities often only achieve partial removal of emerging contaminants (20–70% for most pharmaceuticals/PPCPs) (Grandclément et al., 2017; Miklos et al., 2018). An advanced oxidation process may serve as an effective method for eliminating these persistent organic contaminants from water. However, adding standard advanced oxidation processes to present drinking water treatment facilities is costly, increases the size of the facility, and may lead to high operating costs because of higher energy expenditures. The interaction of chlorine with UV light in water treatment has the potential to transform current chlorine-based disinfection methods into advanced oxidation processes. The photolysis of HOCl and OCl^- generates a range of reactive oxidants, such as •OH, chlorine radical ($Cl^•$). Chlorine photolysis has the potential to effectively inactivate chlorine-resistant pathogens while transforming organic contaminants of concern through a combined approach (Remucal & Manley, 2016).

- Direct reaction with HOCl/ OCl^-.
- Direct photolysis by UV radiation.
- Indirect photolysis caused by reactive species (such as reactions with •OH, Cl•, and/or ClO• generated during chlorine photolysis)

The UV/chlorine process combines the photolysis of free chlorine species (hypochlorous acid, HOCl, and hypochlorite ion, OCl^-) with UV irradiation to produce reactive chlorine species (RCS) and hydroxyl radicals (Type et al., 2024):

$$HOCl + h\nu \rightarrow \bullet OH + Cl\bullet \quad (6)$$

$$OCl^- + h\nu \rightarrow O^-\bullet + Cl\bullet \quad (7)$$

$$Cl\bullet + H20 \rightarrow \bullet OH + HCl \quad (8)$$

This makes the process very effective in the oxidation of the organic compounds since the oxidation is done by two oxidants. In their study, Khajouei et al. (2022) concluded that the process provides higher reaction rates of contaminants compared to UV/H_2O_2 particularly when ammonia or nitrogenous organic compounds are present. However, there are some disadvantages in the formation of chlorinated by-products such as chlorate, trihalomethanes, haloacetic acids, which are health affecting if controlled by proper dosing or optimizing the reaction time.

UV/Persulfate System

In this process, persulfate ions ($S_2O_8^{2-}$) are activated by UV light to form sulfate radicals ($SO_4\bullet^-$), which have a redox potential of approximately 2.6 V and a longer half-life than hydroxyl radicals:

$$S_2O8_2^- + h\nu \rightarrow 2SO_4\cdot^- \quad (9)$$

Sulfate radicals exhibit selective oxidation characteristics and perform well in matrices where •OH may be less effective due to scavenging. Based on the findings of Guerra-Rodríguez et al. (2018), UV/persulfate processes are specifically efficient for the oxidation of high electron density centers such as aromatic ring. They also possess high robustness in high ionic strength

and have potential application in industrial wastewaters environment. However, the cost of persulfate and forming a stable oxidizing agent is still the concern of operation. Besides, the activity of sulfate radical is dependent on the pH; they are best activated and stabilized under neutral to slightly acidic environments.

UV/Ozone System

The synergistic use of UV light and ozone (O_3) enhances the generation of both hydroxyl and other reactive oxygen species (ROS) such as singlet oxygen and ozonide radicals:

$$O_3 + h\nu \rightarrow O_2 + O(^1D) \quad (10)$$

$$O(^1D) + H_2O \rightarrow 2HO \quad (11)$$

This process has high oxidation efficiency and is preferably applicable for the treatment of complicated organic compounds such as pharmaceuticals and industrial dyes (Liu et al., 2018). Nonetheless, UV/ozone systems might face several limitations resulting from their operational mechanism and issues associated with handling the compound ozone and the off gas. However, high ozone doses can form bromate in bromide-containing waters and this requires effective controlling measures.

2.3.3 Why UV/H_2O_2 and UV/Cl_2 Processes Used

The UV/H_2O_2 advanced oxidation process (AOP) has gained wide attention for its high efficiency in degrading both organic and inorganic pollutants. This process offers a major advantage over conventional oxidation methods, such as ozonation, due to its low production of harmful by-products and environmentally friendly operation. The UV/H_2O_2 system is also highly adaptable and can be effectively applied in drinking water treatment, wastewater

purification, and industrial effluent management. Its simple operation and low maintenance requirements, especially compared to ozone-based systems, make it a practical and cost-effective option for routine water treatment applications.

Recently, there has been growing interest in the UV/Cl_2 process for its dual capability in organic contaminant oxidation and microbial disinfection. This makes it particularly suitable for systems where both treatment goals are required simultaneously. However, a key limitation of the UV/Cl_2 process is the formation of chlorinated disinfection by-products (DBPs) during the photolytic degradation of chlorine in the presence of natural organic matter (NOM). Common DBPs reported in UV/Cl_2 systems include trihalomethanes (THMs) such as chloroform ($CHCl_3$), haloacetic acids (HAAs) like dichloroacetic and trichloroacetic acids, as well as chlorate (ClO_3^-), chlorite (ClO_2^-), and N-nitrosodimethylamine (NDMA) a potent carcinogen that can form in the presence of chloramines (Liu et al., 2021).

Overall, both UV/H_2O_2 and UV/Cl_2 processes represent advanced and flexible treatment technologies capable of efficiently removing persistent pollutants. However, the potential formation of harmful by-products in UV/Cl_2 systems highlights the continued importance of optimizing and improving UV-based AOPs for safer and more sustainable water treatment.

2.3.4 Overview of Different Light Sources

Choosing the right light source is critical since it is a key part of light-induced advanced oxidation processes (photochemical reactions). Technical details and the cost are two main factors to consider when selecting a light source. The light source needs to emit photons that can be used directly or indirectly by the target compound. It is essential that the emission spectrum of the light source aligns with the absorption spectrum of the reactants, which could be either the target organic compound or the oxidants. UV lamps used in this study are broadly classified into low-pressure and medium-pressure systems. Comparative LP vs MP

performance under aeration remains unstudied despite spectral differences affecting $HOCl/OCl^-$ photolysis..

Low-Pressure UV Lamp

Low-pressure (LP) mercury vapor UV lamps are widely used in water treatment because they're energy-efficient, affordable to operate, and consistently effective at disinfecting microbes and breaking down micropollutants, especially when operating conditions are well managed. These lamps mainly emit UV light at a wavelength of 254 nanometers (see figure 1.), with more than 85–90% of their energy concentrated at this specific point (Lagunas-Solar, 2014). This narrow focus makes them especially good at triggering photolytic reactions with oxidants like hydrogen peroxide and chlorine, which absorb light strongly at 254 nm. However, this limited emission range also presents a drawback: it makes the lamps less effective for activating other photocatalysts or oxidants that require different wavelengths to work properly (Ijpelaar et al., 2010). So, while low pressure UV systems perform very well under certain conditions, their narrow spectral range can limit how broadly they are used in more advanced oxidation processes.

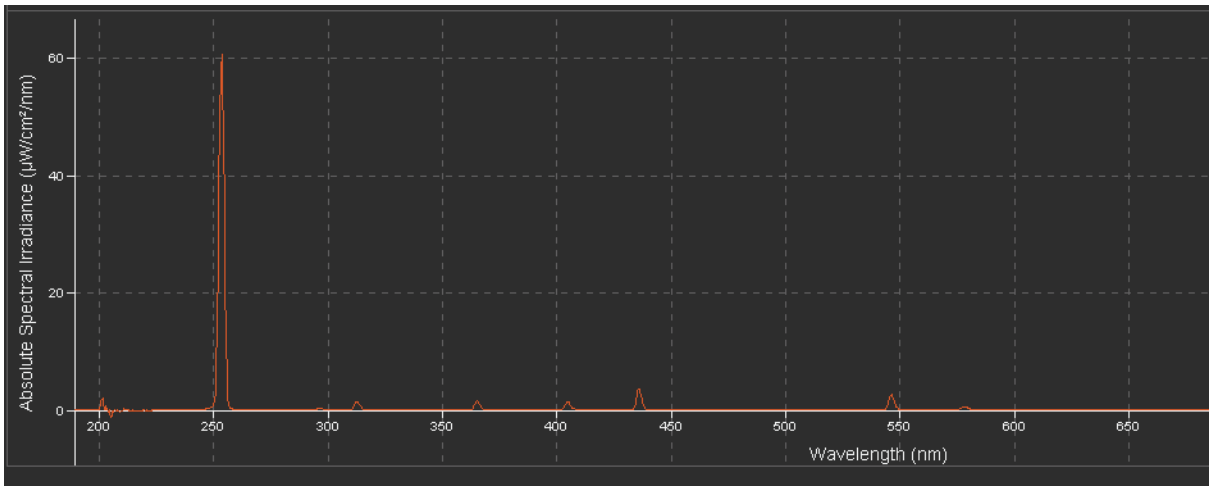

Figure 1. Low-pressure UV lamp spectrum with Ocean View application

Medium-Pressure UV Lamps

Medium-pressure ultraviolet (MP) lamps can emit a wide spectrum of ultraviolet light, which generally falls within the range of 200 to 400 nanometers. This polychromatic emission profile makes it possible to activate numerous oxidants at the same time and improves the degradation of a larger variety of pollutants, which ultimately results in an increase in the overall effectiveness of advanced oxidation processes (Ijpelaar et al., 2010). The disadvantages, on the other hand, include a decrease in energy efficiency and an increase in the difficulties associated with operations. Medium-pressure lamps produce a substantially higher amount of heat, which can result in thermal stress, faster wear on equipment, and increased maintenance requirements. Therefore, the choice between low-pressure and medium-pressure ultraviolet (UV) systems needs to be led by a complete review of criteria such as the amount of energy consumed, the costs of operation, the durability of the system, and the pollutant removal goals of the treatment process. Figure 2. shows the medium pressure UV spectrum.

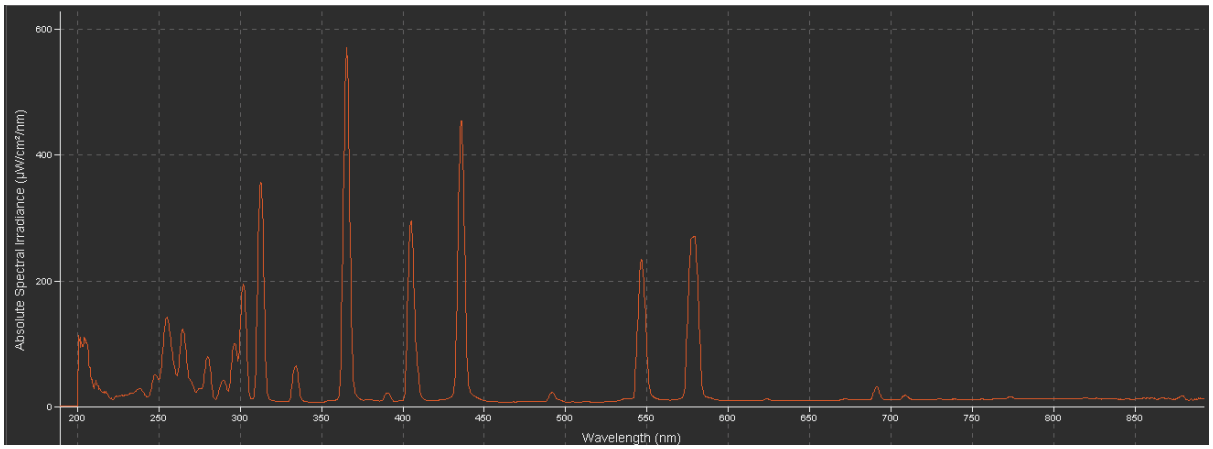

Figure 2. Medium Pressure UV Lamp spectrum with Ocean View software.

2.4 Photon Management and Design Constraints in Conventional UV Reactors

Although UV reactors exhibit significant effectiveness in controlled laboratory settings, their performance frequently declines when implemented in full-scale water treatment. The variation occurs mainly from various engineering and operational challenges that influence the

consistent delivery and absorption of UV fluence. A significant limitation is the inefficient use of generated UV photons. In practical applications, elements like lamp fouling, reactor geometry, flow dynamics, and water matrix composition can considerably reduce the intensity and distribution of UV light. A significant fraction of emitted photons may be lost due to reflection, absorption by non-target constituents, or insufficient mixing, which diminishes the system's oxidative potential and overall treatment efficacy. Scale-up from lab to full-scale introduces complexities including reactor pathlength variations, flow regime transitions (laminar to turbulent), and wall effects that diminish photon recovery (Bolton & Stefan, 2002).

2.4.1 Photon Utilization Inefficiencies

In traditional UV reactors, a significant number of photons is lost prior to reaching target contaminants, thereby reducing process efficiency. The losses arise due to scattering by suspended solids, and absorption by reactor walls or materials such as quartz sleeves and stainless steel. According to Cantwell and Hofmann (2011), depending on the reactor geometry and water quality, as much as 40–70% of UV photons can be lost before participating in photochemical reactions. Li et al. (2012) reported that approximately 40–50% of UV photons at 254 nm are absorbed by reactor walls, while Chen et al. (2021) observed that 70–80% of photons at 300 nm are similarly lost due to wall absorption One major problem is the limited optical pathlength (1–5 cm), which restricts the amount of photons that may be absorbed by pollutants or oxidants. Penetration depth may go below 2 cm in murky or colorful waters with UVT < 80%, making the issue worse (Tedetti & Sempéré, 2006). UV fluence, measured in mJ/cm^2, represents the energy imparted per unit area. Micropollutants characterized by low reactivity typically require 500–1000 mJ/cm^2 for effective degradation. Nonetheless, inadequate photon utilization can result in a reduction of actual fluence by more than 50%, causing incomplete treatment and energy loss (Tedetti & Sempéré, 2006). The identified

inefficiencies demand the necessity for enhanced reactor design, including improved reflectivity, optimized flow, and advanced light delivery methods, to increase photon utilization and treatment efficacy.

2.4.2 Role of Light Path-length

The light path-length refers to the distance UV photons travel within a reactor before being absorbed or escaping the system. A longer optical path-length allows photons to interact more frequently with oxidants, thereby enhancing the formation of reactive species and improving the overall efficiency of photochemical reactions (Bolton & Stefan, 2002). Conversely, in many conventional UV reactors, the optical path-length is short, meaning photons pass rapidly through the medium with limited interaction, which reduces treatment efficiency (Autin et al., 2013). Several approaches have been explored to increase the effective light path-length, including modifying reactor geometry and incorporating internal reflectors to extend photon trajectories (Mbonimpa et al., 2012). Modeling efforts based on the Beer–Lambert Law and radiative transfer equations have shown that pathlength strongly influences reactor performance (Parnis & Oldham, 2013). More recently, Jaimes-López et al. (2024) and Han et al. (2022) demonstrated both theoretically and experimentally that reactors with longer light pathlengths achieve higher •OH radical generation and greater micropollutant degradation rates, confirming the critical role of optical path-length optimization in UV-based AOP systems.

2.4.3 Use of Reflective Materials in UV Reactors

Reflective materials have been widely studied to improve the efficiency of UV reactors by redirecting photons that would otherwise be absorbed by the reactor walls. Using highly reflective surfaces, such as polished aluminum, can significantly enhance the effective UV fluence within the reactor by up to 90%, as reported by He(Heidarinejad et al., 2020). Similarly,

Li et al. (2017) demonstrated that internal reflective coatings improve photon retention and, consequently, increase contaminant degradation efficiency. Further research compared different reflector materials and geometries to optimize performance. (Heidarinejad et al., 2020) observed that while polished aluminum provides notable improvements initially, its reflectivity declines over time due to fouling and surface degradation. (Martín-Sómer et al., 2023) emphasized that although reflective materials enhance reactor performance under controlled laboratory conditions, their long-term effectiveness in real water systems depends on resistance to fouling and stability under complex water qualities

2.4.4 Limitation of Reflective Materials

Despite their benefits, reflective materials face several practical limitations. The main issue is biofouling, where microorganisms, organic matter, and scaling form a layer on the reflective surface, reducing its ability to reflect light (Zhao & Yu, 2015). Frequent cleaning or replacement is often required, which adds maintenance costs and can interrupt system operation. Moreover, in turbid or colored water, the advantage of using reflectors is reduced since most photons are absorbed by dissolved substances before they can be reflected (Al-Nuaim et al., 2022). There are also material limitations reflective coatings can only partially recover photons lost to wall absorption, meaning not all light can be reused effectively (Shanmugam et al., 2020). Overall, while reflective materials can enhance photon use in UV reactors, their long-term effectiveness is often limited by fouling, maintenance needs, and changing water conditions.

2.4.5 Rationale for Aeration-Assisted UV AOPs

According to Cantwell and Hofmann (2011), depending on reactor geometry and water quality, 40–70% of UV photons can be lost before they participate in photochemical reactions. Similarly, (W. Li et al., 2017) reported that about 40–50% of UV photons at 254 nm are

absorbed by reactor walls. To address these high photon losses and improve reactor efficiency, aeration has emerged as a promising approach. Introducing air bubbles into a UV reactor can enhance photon utilization through light scattering and reflection. Scattering occurs when photons encounter interfaces between materials with different refractive indices, such as air and water, causing them to deviate from their original path. Reflection happens when photons strike bubble surfaces and bounce back into the reactor instead of being absorbed or escaping. Together, these phenomena increase the effective path length and retention time of photons, improving the likelihood of interactions with target contaminants or reactive species, and thereby enhancing the overall photochemical efficiency compared to systems without bubbles.

2.4.6 Innovative Concept of Air Bubble Integration

The integration of air bubbles within a UV reactor is hypothesized to create numerous air–water interfaces, which act as reflective and scattering boundaries for UV photons, effectively trapping them within the water column and reducing losses to the reactor walls (Miletta et al., 2011). In a reactor without aeration, most photons travel in nearly straight paths and are often absorbed by the reactor walls, limiting their interaction with oxidants. When air bubbles are present, photons encounter multiple interfaces that redirect and reflect them, resulting in increasing the path-length and retention time. These longer paths increase the likelihood that photons will interact with oxidants rather than being lost, enhancing the overall photochemical efficiency (Vilanova et al., 2024). This mechanism can be illustrated with a simple scheme: consider a reactor with water and UV lamp is placed at the center. In a non-aerated system, a significant fraction of the emitted photons is absorbed by the walls, contributing less effectively to photochemical reactions. By contrast, when air is introduced through a diffuser, the water is filled with dispersed small air bubbles. These bubbles function like reflective surfaces, scattering photos and keeping them within the reactive zone of the reactor for longer periods.

As a result, photon utilization increases, which enhances the degradation efficiency of micropollutants. The concept of how bubbles scatter and reflects the photons can be explained by figure 3.

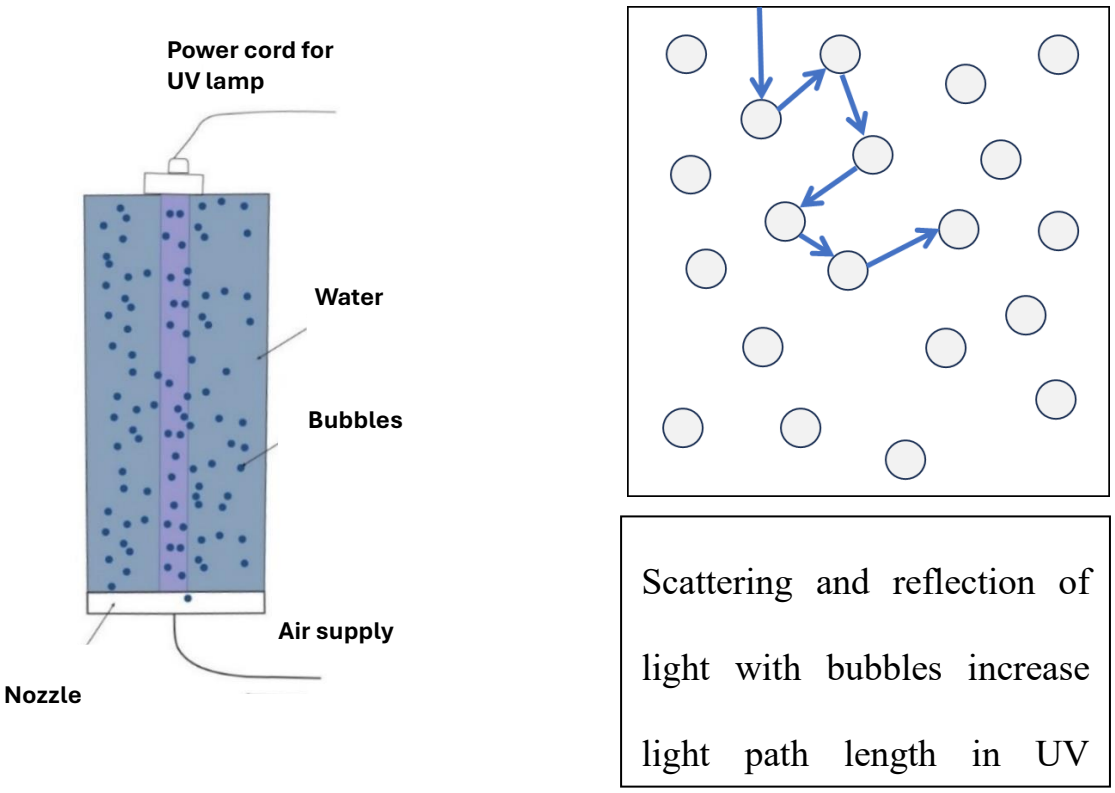

Figure 3.Schematic diagram of reflection and scattering of light (photons) with bubbles present in an aqueous medium.

2.5 Secondary Benefits of Aeration

Apart from its primary function of enhancing photon utilization, the aeration-assisted approach offers additional advantages:

2.5.1 Volatilization and Stripping of Intermediates and By-products

Aeration introduces a continuous flow of microbubbles into the water, which promotes the volatilization of dissolved gases and volatile organic compounds. This process, known as gas

stripping, plays a key role in removing potentially harmful by-products formed during the oxidative breakdown of micropollutants. Compounds such as chloroform, trihalomethanes (THMs), and volatile aldehydes, which can result from the partial oxidation of aromatic or halogenated organics, can be effectively eliminated from the water through this mechanism (Miklos et al., 2019). In this way, aeration contributes to the control of secondary pollution, improves overall water quality, and reduces the residual toxicity in treated effluents.

2.5.2 Biofouling and Scaling Mitigation

The upward motion of air bubbles introduces turbulence and localized shear forces at the fluid–solid interface within UV reactors. This hydrodynamic activity minimizes the chances of biofilms formation and scaling of the quartz sleeves and reactor wall, which is normally used to cover UV lamps. Since the bubbles rise and rupture frequently, they maintain a high rate of surface renewal, which helps prevent fouling processes such as calcium carbonate scaling, iron deposition, and microbial attachment on surfaces.(Sisay et al., 2023). It maintains the UV transmittance through protective sleeves while at the same time enhancing the durability of the reactor parts and decreasing the time between the maintenance intervals.

2.6 Generation and Quantification of Microbubbles

2.6.1 Introduction

Microbubbles are gas bubbles with diameters of 10-100 micrometers that got a lot of attention in recent years due to the unique properties and wide spectrum of the applicability in different industrial processes, primarily in water treatment, chemical reactions, flotation, wastewater treatment, and food processing (Zhou et al., 2022). Small size and high ratio of the surface to volume make them able to enhance the efficiency of several processes: chemical reaction, flotation of particles, and even processing of wastewater (Azevedo et al., 2016). For the case

of advanced oxidation processes (AOPs), microbubbles are applied to increase the utilization of the photons and production of reactive species such as hydroxyl radicals, which are very powerful in the breakdown of organic pollutants (Rekhate & Srivastava, 2020). Microbubbles are especially efficient in the improvement of the ultraviolet (UV)-based AOPs' performance. In UV based reactors, the main role of microbubbles is to increase the distribution of UV photons in water, enhance the UV photons retention time inside the reactor by increase their travelling distance, instead of going straight inside the reactor UV photons move zig zag after scattering and reflecting from the surface of bubbles. These effects enhance the interaction of the pollutants with the UV light and thereby increase the degradation rate of the contaminants in the treated water. Given this, combining microbubbles with UV irradiation in reactors is a great approach to augmenting the efficiency of water and wastewater treatment processes (Gao et al., 2019; John et al., 2020).

2.6.2 Application of Microbubbles

Microbubbles have proven highly valuable in water and wastewater treatment due to their large surface area-to-volume ratio, which enhances gas–liquid interactions. This property significantly improves processes such as aeration, flotation, and disinfection. In aeration, microbubbles enhance oxygen transfer by increasing contact between oxygen and microorganisms (Kizhisseri et al., 2025). During flotation, they help lift suspended solids and contaminants for removal (Ran et al., 2013). In disinfection, microbubbles improve contact between disinfectants (e.g., ozone) and microorganisms, resulting in more efficient microbial inactivation (Azevedo et al., 2016).

Among their many applications, microbubbles are particularly beneficial in advanced oxidation processes (AOPs), where they enhance the generation of reactive oxygen species (ROS) that break down persistent organic pollutants. Their small size and high gas-to-liquid ratio enable

better mass transfer and more effective use of oxidants, ultimately improving pollutant degradation and disinfection efficiency. In UV-based AOPs, one major limitation is photon wastage, UV light absorbed by the reactor walls reduces treatment efficiency (Gopalakrishnan et al., 2023). Microbubbles help overcome this issue by introducing numerous dynamic air–water interfaces that scatter and reflect UV photons. This scattering increases photon path length and residence time, giving oxidants more opportunities to absorb light and produce hydroxyl radicals, the primary agents responsible for pollutant degradation (Pera-Titus et al., 2004). Furthermore, as microbubbles travel through the reactor, photons continuously reflect off their surfaces, effectively extending the light pathlenght within the water column. This enhanced photon retention time and improved the utilization of UV photon and accelerates the breakdown of low concentration micropollutants, such as pharmaceutical residues and industrial chemicals that resist conventional treatment (Cesaro & Belgiorno, 2016; Takahashi et al., 2012). Overall, the integration of microbubbles in UV-AOP systems significantly enhances photon efficiency, reactive species generation, and pollutant degradation performance. However, no studies currently quantify how microbubble concentration and flow rate affect oxidant decay in UV-AOP reactors, which is a critical gap in understanding the optimal conditions for improving reactor performance

Beyond conventional water treatment, microbubble technology has demonstrated remarkable potential in the treatment of industrial, agricultural, and environmental wastewaters. Industrial effluents from manufacturing, textile, and chemical processing plants often contain complex and persistent pollutants such as heavy metals, dyes, and organic solvents that are difficult to remove through traditional methods (Patel et al., 2025). In sludge management and resource recovery, microbubbles improve flotation-based separation processes, enhancing sludge thickening and dewatering efficiency (Anyame Bawa et al., 2024).

Emerging research are increasingly focused on integrating microbubbles with advanced treatment technologies such as membrane filtration, photocatalysis, and electrochemical oxidation (Fan et al., 2021; Mwanga et al., 2024; Ning et al., 2024). These hybrid systems aim to exploit the unique physicochemical properties of microbubbles to achieve higher treatment efficiencies and lower operational costs (Nishu & Kumar, 2023). Furthermore, innovations in low-energy, cost-effective microbubble generation techniques are essential for scaling up their application from laboratory research to full-scale industrial and municipal systems (Gao et al., 2024). But,

2.7 Methods for the Generation of Microbubbles

2.7.1 Overview of Bubble Generation Methods

Microbubbles can be generated within water treatment systems using a variety of techniques, each offering specific benefits and limitations depending on the operational conditions and treatment objectives. Common methods for microbubble generation include mechanical diffusers, Venturi injectors, cavitation-based systems, and nanobubble generators (Lee et al., 2019). (Table 4) shows the comparison of bubble generation methods.

Table 4. Comparison of Bubble Generation Methods

Bubble Generation Method	**Mechanism of Bubble Generation**	**Advantages**	**Disadvantages**
Mechanical Diffusers	Gas is forced through fine pores or porous membranes, forming bubbles as it exits into the liquid.	Simple design, low cost, easy operation, widely used in water treatment applications.	Produces relatively larger bubbles; limited control over bubble size distribution
Venturi Injectors	Gas is entrained into liquid through a constricted Venturi throat, creating shear and turbulence that generate bubbles	Can produce smaller bubbles; improved gas–liquid contact; no moving parts, reducing maintenance needs.	Requires continuous pressure input; potential clogging issues; moderate operating cost
Cavitation-based Systems	Rapid pressure fluctuations create vapor cavities that collapse violently, forming bubbles and micro-jets	Generates extremely fine bubbles; high mass-transfer efficiency; suitable for strong mixing and contaminant breakdown.	High energy consumption; complex equipment; cavitation erosion and maintenance challenges.
Nanobubble Generators	Specialized devices create ultra-fine, stable nanobubbles through mechanical or hydrodynamic mechanisms.	Produce stable nanobubbles with high surface area and enhanced reactivity; long residence time in water.	Higher capital cost; advanced technology; challenges with large-scale implementation.

Each of these approaches operates based on distinct physical principles and is associated with operational advantages and challenges. The selection of an appropriate method depends on several factors, such as the scale of the treatment system, the target bubble size, and the intended application whether it be aeration, contaminant removal, or enhancement of advanced oxidation processes.

Mechanical Diffuser

Mechanical diffusers, such as porous ceramics and sintered glass, are widely used for generating microbubbles due to their simplicity and reliability. These devices use the process of passing air or gas through porous materials to make bubbles which then cause gas to be

distributed into the water as fine bubbles. The sizes of the bubbles can be regulated from controlling parameters like pore size of the material of the diffuser and gas flow rate. Nevertheless, one weakness of mechanical diffusers is that it forms bubbles with a wide size distribution where this may not be suitable for uses that require varying sizes of bubbles (Kukizaki & Baba, 2008).

Venturi Injector

Venturi injectors, which utilize the Venturi effect, are another common method for generating microbubbles. These devices use a constriction in the flow path of water to create a drop in pressure, causing air to be drawn into the water stream. The air is then sheared off into fine bubbles by water accelerating through the small injector. Venturi injectors can produce microbubbles of a rather narrow size spectrum, and they can be employed to produce bulk amounts of bubbles with high efficiency. But their effectiveness is dependent on flow rate of the water pressure, as they may not be applicable in some of the systems due to their limits (Baylar & Ozkan, 2006).

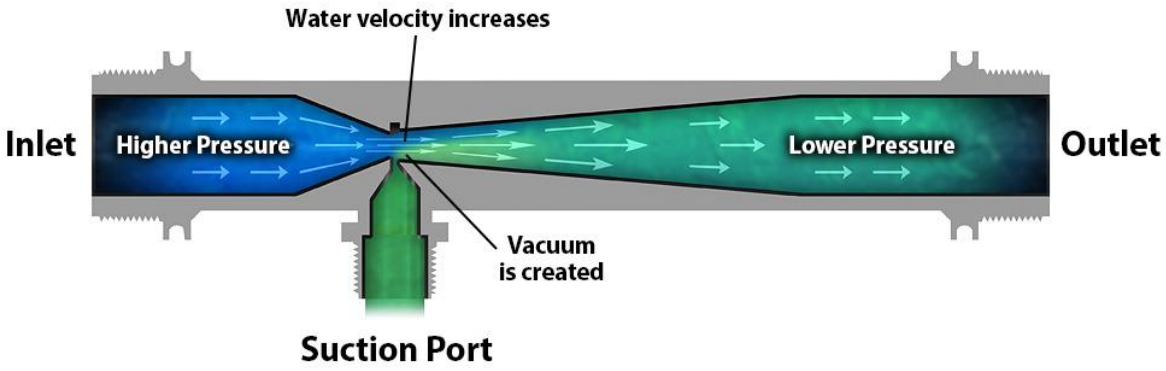

Figure 4. Schematic diagram of venturi injector (Lauria & Company, 2019)

Swirl Flow Method

In this current research, the swirl flow method was selected for generating fine bubbles. This technique involves introducing water or a water air mixture tangentially into a cylindrical vessel, thereby inducing a strong rotational or swirl flow within the chamber. The resulting vortex generates a region of low pressure along the central axis of the vessel, which passively draws air from an inlet at the top. As the swirling flow develops, the entrained air column is subjected to intense shear forces, particularly in the outer regions of the flow near the bottom or outlet of the vessel. These shear forces fragment the air column into fine bubbles, effectively dispersing them throughout the liquid phase.

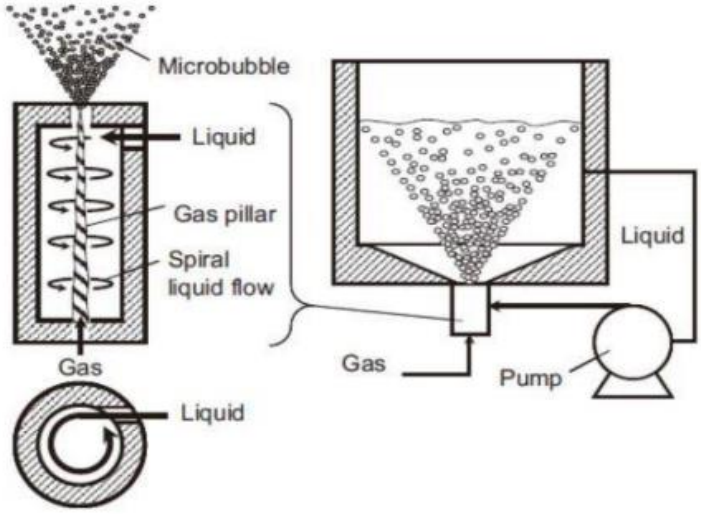

Figure 5. Top view of Spiral liquid flow generation method (H. Li et al., 2013).

2.8 Quantification of Microbubbles

The performance of microbubble-based treatment systems is strongly influenced by the size distribution of the bubbles, so the quantification of bubbles is a critical factor (Wang et al., 2015; Etchepare et al., 2017). Microbubbles, typically ranging from 10 to 100 μm, exhibit distinct behaviors depending on their diameter: smaller bubbles rise more slowly and remain

suspended longer, allowing extended interaction with contaminants, improved gas dissolution, and enhanced mass transfer (Agarwal et al., 2011). Techniques for measuring bubble size and concentration such as optical imaging, laser diffraction, and acoustic methods provide essential information about their distribution, stability, and overall efficiency within water treatment systems. Precise control over bubble size is particularly important in processes like dissolved air flotation (DAF) and advanced oxidation, where the probability of bubble–particle or bubble–oxidant interactions directly impact contaminant removal efficiency (Ahmed et al., 2018; Calgaroto et al., 2015). Smaller, uniform bubbles generate larger interfacial areas and prolonged residence times, optimizing both flotation performance and reactive species generation.

2.8.1 Detection Techniques for Microbubbles

Laser Diffraction Scattering Method

In the laser diffraction method, when a beam of light encounters a particle, the light is either diffracted or scattered, depending on the size and nature of the particle. The pattern and intensity of this scattering or diffraction are influenced by the particle size. Generally, larger particles scatter light at smaller angles with greater intensity, while smaller particles scatter

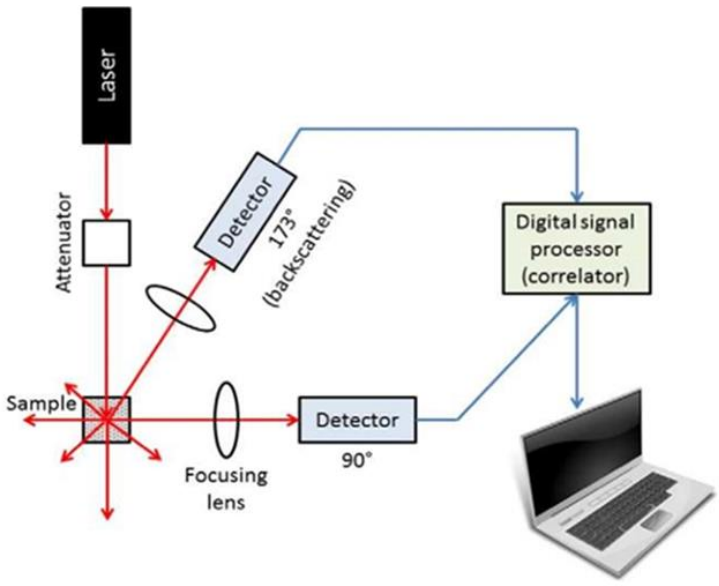

light at wider angles with less intensity. The instrument records the scattering intensity at various angles, and from this data, the particle size distribution is calculated. This calculation is typically performed using mathematical models such as the Fraunhofer diffraction model or the Mie scattering theory (Bittelli et al., 2022). Mie scattering theory is more suitable for

Figure 6. Schematic showing the instrumentation of Laser Diffraction Scattering (Bhattacharjee, 2016).

bubbles due to their transparent nature and size range comparable to the wavelength of light, as it accounts for refractive index and precise scattering mechanisms, while Fraunhofer diffraction is an approximation valid primarily for large, opaque particles at small scattering angles.

Particle Tracking Analysis Method

The Particle Tracking Analysis (PTA) technique commonly referred to as Nanoparticle Tracking Analysis (NTA) combines the principles of light scattering and Brownian motion to measure particle size distribution and particle concentration in liquid samples in real time. In

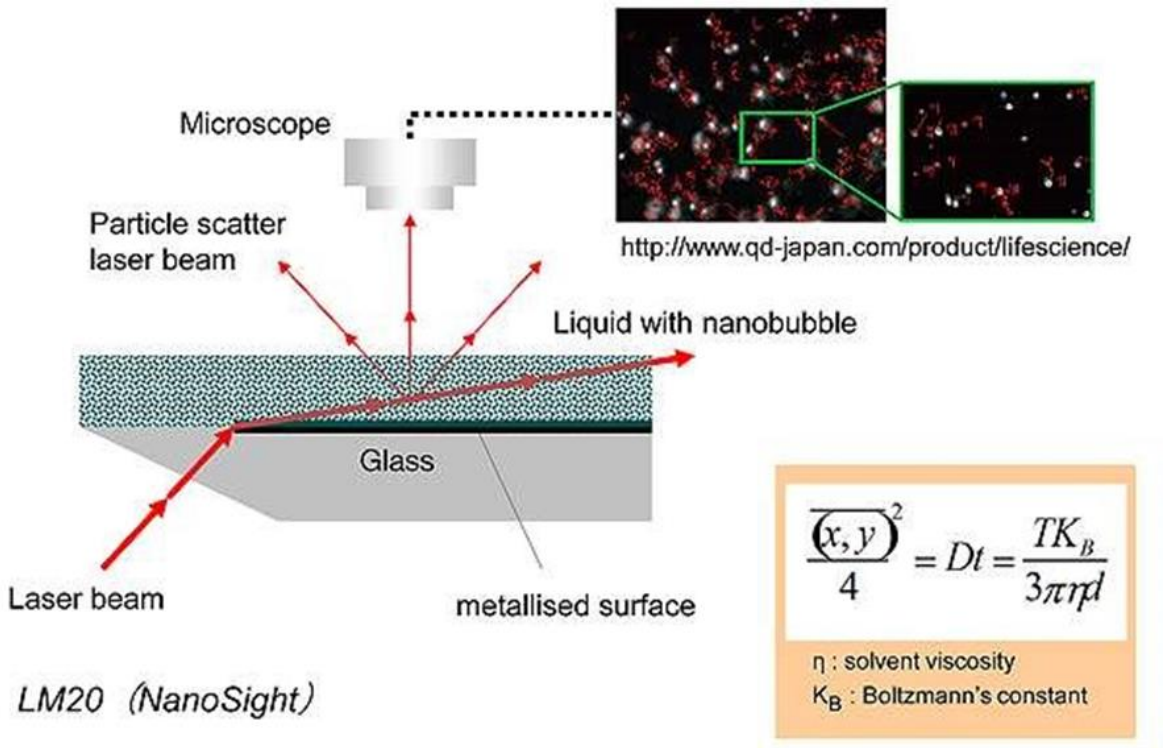

this method, particles suspended in a fluid are illuminated, typically by a laser, and the scattered light is captured using a microscope equipped with a camera. The particles movement, caused by Brownian motion, is tracked over time. Since the speed of this motion is inversely related

Figure 7. Particle tracking analysis method (Bhattacharjee, 2016).

to particle size (i.e., smaller particles move more rapidly than larger ones), the software analyses each particle's trajectory to calculate its hydrodynamic diameter. This allows the system to generate both size distribution and particle count data simultaneously.

2.9 Decay of Oxidants

2.9.1 Introduction

Advanced Oxidation Processes (AOPs) have gained significant attention in recent years as effective technologies for water and wastewater treatment due to their strong potential to degrade a broad spectrum of organic pollutants. Among the various AOPs, ultraviolet (UV)-based systems stand out because of their ability to generate highly reactive oxygen species (ROS), particularly hydroxyl radicals (•OH), which are capable of rapidly oxidizing the most persistent contaminants (Pera-Titus et al., 2004). Among the various AOPs, ultraviolet (UV)-based systems such as UV/H_2O_2 and UV/Cl_2 are widely employed due to their simplicity, high reaction rates, and ability to operate without additional catalysts (Hübner et al., 2024). Despite their proven effectiveness, the performance of UV-AOP systems is often limited by photon losses within the reactor. UV light can be absorbed, reflected, or refracted by reactor walls and surfaces before interacting with the target oxidants, reducing the fraction of photons available for photolysis and radical formation (Meng et al., 2023). Consequently, improving photon utilization efficiency remains a major challenge for optimizing UV reactor design and

operation. Recent studies have explored the introduction of microbubbles into UV systems as a novel means to enhance photon efficiency. Microbubbles, gas bubbles typically ranging from 10 to 100 μm in diameter exhibit unique optical and physical properties that distinguish them from conventional millimeter-sized bubbles. Their large surface area and high refractive index contrast with water allow them to scatter and reflect UV photons, effectively extending photon residence time within the reactor and increasing the likelihood of photon–oxidant interactions (Takahashi et al., 2007) . In addition, microbubbles contribute to localized turbulence and improved mixing, which enhances oxidant contact with reactive zones (dark zone areas) and promotes radical formation (Ning et al., 2025)

Building upon these findings, this study investigates the influence of microbubble (aeration) on the degradation of hydrogen peroxide (H_2O_2) and chlorine (Cl_2) in a continuous-flow UV reactor. Specifically, the objectives of this research are to:

- Determine the baseline degradation rates of H_2O_2 and Cl_2 under non-aerated (control) conditions.

- Evaluate how varying microbubble concentration influence oxidant decay rates with different flow rates.

- Compare the performance of low-pressure (LP) and medium-pressure (MP) UV lamps in promoting oxidant degradation rates under non-aerated and aerated conditions.

- Quantify photon utilization efficiency using the enhancement ratio (k_{air} / $k_{no\text{-}air}$).

Through these objectives, a proof of concept for microbubble-enhanced UV-AOPs and how aeration-induced photon scattering can intensify oxidant degradation and overall reactor performance will be verified.

2.10 Micropollutants

2.10.1 Introduction

Micropollutants in water are a growing concern for modern water treatment systems because they are often persistent and difficult to remove using conventional processes (Nishmitha et al., 2025). These contaminants, which include pharmaceuticals, personal care products, and industrial chemicals, can accumulate in aquatic environments and enter the food chain, posing potential risks to both ecosystems and human health (Pavi et al., 2025). In this study, the degradation of three representative micropollutants, caffeine, benzoic acid, and nitrobenzene was investigated using a microbubble-enhanced UV-based advanced oxidation process (UV-AOP). These compounds were specifically selected because of their different reactivity toward oxidant-derived radicals, which makes them ideal model pollutants for comparing process performance. Caffeine was selected because it reacts readily with hydroxyl radicals (•OH) and chlorine radicals (Cl•), representing compounds that are highly susceptible to UV-AOP treatment. Benzoic acid was chosen as a moderately reactive compound that has been widely studied in previous UV-based oxidation research (UV/H_2O_2 and UV/Cl_2), providing a useful benchmark for comparison (Sharpless & Linden, 2003; Fang et al., 2014)Nitrobenzene was selected as a more resistant compound because it reacts primarily with hydroxyl radicals and shows limited reactivity with chlorine-based radicals, making it a good model for persistent pollutants. By selecting these three compounds with contrasting reactivities, this study was able to systematically evaluate how oxidant dosage (5 mg/L vs. 10 mg/L), UV lamp type (LP vs. MP), and microbubble concentration influence the degradation behavior of micropollutants.

2.11 Research Gaps and Justification

Although UV-based advanced oxidation processes (AOPs) have proven effective in treating micropollutants, several important challenges still limit their overall efficiency, particularly at full scale. One major issue is the inefficient use of UV photons. A large portion of the photons generated in conventional reactors never reach the target pollutants; instead, they are lost due to absorption by reactor walls or scattering by non-target materials in the water. Research has shown that as much as 70% of photons may be lost before participating in any useful reactions (Cantwell & Hofmann, 2011; Chen et al., 2021). While reflective materials have been used to reduce these losses, their performance often declines over time due to fouling and material degradation (Wang et al., 2011).

An approach that has received little attention is the use of microbubbles to improve light behavior inside UV-AOP reactors (Ning et al., 2024; Hutagalung et al., 2023). Although bubbles are commonly used for aeration or mixing, their ability to reflect and scatter UV light in water treatment systems is not well studied (Ning et al., 2024; Miklos et al., 2018). The presence of air–water interfaces can help redirect photons back into the water, increasing their chances of reacting with oxidants and pollutants by increasing the path length. Some earlier work has mentioned this concept (Miletta et al., 2011; Vilanova et al., 2024) but lacks systematic experimental validation of photon pathlength enhancement and treatment kinetics in UV-based AOPs (Ning et al., 2024). No standardized metric exists to quantify aeration-enhanced photon utilization ($k_{air}/k_{no\text{-}air}$), which is a critical gap in understanding how aeration improves UV-AOP performance. This research addresses that gap by directly testing how aeration influences photon movement and improves treatment efficiency. Another limitation in past studies is the lack of focus on bubble characteristics. Few researchers have examined how bubble size distribution (10-100 μm), concentration, or stability affect light scattering (Wang

et al., 2015). By studying these parameters, this research adds valuable insights on how to find optimum microbubble conditions to boost the treatment.

Most research tends to treat light behavior and chemical reactions separately (Miklos et al., 2018). This study integrates photon pathlength modeling with measured ($k_{air}/k_{no\text{-}air}$ ratios) for oxidants/micropollutants. But if photons stay in the reactor longer due to better scattering, they have more chances to interact with oxidants and generate radicals. This could lead to faster degradation of pollutants. However, this potential connection hasn't been deeply explored. This study looks at both sides how light moves in the reactor and how that affects oxidant decay and pollutant breakdown helping to close this knowledge gap (Miklos et al., 2018; Wang et al., 2019).

Lastly, common approaches to improve photon efficiency, such as using reflective coatings, often lead to maintenance challenges due to fouling or scaling. Microbubbles may offer a cleaner, more passive solution. Besides improving photon use, aeration also creates gentle turbulence that can reduce the buildup of scale and biofilms on reactor surfaces. This dual benefit, optical and operational, makes microbubble-assisted UV systems an attractive solution for improving both performance and durability over time. In short, this research responds to several key limitations in current UV AOP technology by introducing a simple, yet powerful, enhancement technique that improves light use, accelerates treatment, and reduces maintenance filling critical gaps left by earlier studies.

2.12 Conclusion

The literature reviewed in this chapter presents a multifaceted understanding of micropollutants, UV-based advanced oxidation processes, and reactor optimization strategies. Micropollutants are extremely dangerous substances, even at small concentrations, for aquatic

organisms and for human beings as well, which justify the need for highly effective treatment technologies (Sgroi et al., 2021). AOPs, and particularly the ones that involve UV light, have been recognized as effective tools for eradicating most all the pollutants since they create highly reactive species such as hydroxyl radicals (Pera-Titus et al., 2004; Glaze et al., 1987). However, these processes could only be effective if there were optimal consumption of UV photons. Photon absorption and scattering in UV reactors have been widely studied, revealing that both reactor design and water quality are key determinants of performance (Li et al., 2012). Efforts to increase the effective path length of the light which can be achieved through the substrate reflectivity and the reactor design have been evidenced to increase the UV fluence as well as the contaminants removal. While reflective materials have been used to reduce photon losses, problems such as fouling and the associated maintenance requirements of static reflective surfaces have driven research toward dynamic alternatives (Sillanpää et al., 2018). Microbubbles offer a promising solution by continuously scattering photons through air-water interfaces while their motion prevents surface accumulation .

Aeration has emerged as a promising technique not only to enhance oxygenation and mixing but also to improve photon retention in UV reactors. UV light scattering in the air surrounding the bubbles causes expansion of the optical pathlength, thus enhancing the formation of reactive radicals as reported by Takahashi et al., 2012 & Zhao et al., 2015. Computational as well as laboratory analysis has proved that enhanced aeration triggers higher efficiency of UV-AOPs. Nevertheless, there is a lack of extensive studies on bubble dynamics and its application in the design of the reactor. The reviewed studies equally emphasize that it is possible to achieve integration of experimental data, theoretical and computational modeling, and total cost assessment. Some major gaps for the next steps are associated with the bubble parameters optimization, with the geometry and operating conditions' scaling-up from the lab scale to the full-scale applications, and with the absence of the models that combine both optical and

hydrodynamic studies. Thus, the current literature offers a strong background for the research that will further focus on the enhancement of the aeration-assisted UV-based AOPs for micropollutant elimination. Through filling the outlined gaps, this study will help gain improved understanding on the use of photons in the UV reactors, improving on the treatment efficacy and providing economic solutions for the sustainable treatment of water.

CHAPTER 3: METHODOLOGY, RESULTS AND DISCUSSION

This chapter outlines the experimental procedures used to investigate the effects of microbubble aeration on the performance of UV-based Advanced Oxidation Processes. It details the design and operation of the UV reactors, the method of microbubble generation and characterization, and the analytical techniques used to quantify both oxidant decay (hydrogen peroxide and free chlorine) and micropollutant degradation (caffeine, benzoic acid, and nitrobenzene). The chapter then presents the full set of results, beginning with microbubble size distribution, followed by oxidant decay kinetics under aerated and non-aerated conditions, and concluding with the degradation behavior of the selected micropollutants. A comprehensive discussion interprets these findings, linking them to photon utilization efficiency, bubble-induced light scattering, reactor geometry, and oxidant chemistry. Together, these analyses provide a deeper understanding of how microbubble integration enhances the overall treatment performance of UV-AOP systems.

3.1. Reactor Design for UV-Based AOPs

In UV-based advanced oxidation processes (UV-AOPs), the design of the reactor is a critical factor that determines the overall efficiency of contaminant degradation. The geometry of the reactor not only shapes the distribution of UV radiation but also defines the optical path length that photons travel, directly influencing their interactions with pollutants (Rodríguez-Chueca et al., 2023; Martín-Sómer et al., 2023). Longer optical paths generally enhance photon absorption, providing greater opportunities for photochemical reactions, whereas shorter path length may lead to inefficient photon use, as photons may be absorbed by reactor materials before effectively participating in photochemical reactions (Martín-Sómer et al., 2023). Therefore, reactor design is crucial in maximizing the exposure of pollutants to UV light, ultimately improving the efficiency of the oxidation process. Beyond geometry, the

arrangement of UV lamps is essential for ensuring uniform photon distribution throughout the reactor volume; improper lamp positioning can result in non-uniform UV exposure, creating shadowed zones with insufficient radiation, which compromises the overall system performance (Oguma et al., 2016). Additionally, the choice of reactor material significantly impacts photon utilization. Materials with high reflectivity, such as stainless steel, reflect photons that strike the reactor walls back into the water, increasing interactions of UV photons with contaminants and enhancing pollutant degradation (Mei et al., 2023). Therefore, the combined optimization of reactor geometry, lamp positioning, and reflective materials is fundamental to improving photon utilization and achieving effective UV-AOP performance. However, even with those optimizations, the light path length is still limited by the reactor size, and some photons will be wasted due to absorption by reactor materials (e.g., walls and accessories).

Reactor Sizes (d = 20 cm diameter, 50 cm diameter)

A small 20 cm diameter reactor was used to evaluate conditions associated with a short light path. This setup reflects the scale of domestic or home-use UV systems, allowing controlled testing of UV-based AOPs and how different operating conditions influence treatment performance.

In contrast, the 50 cm diameter reactor was selected to represent a longer light path, which is close to the dimensions of commercial UV reactors typically used in water treatment facilities with size of ranging 50 cm to 100 cm (Hu, 2021). This will help assess how the system performs when scaled beyond laboratory settings.

3.1.1 General Design Overview

The reactor used in this study is a cylindrical chamber with a height of 34 cm, enough to accommodate a low-pressure UV lamp (model GPH357T5L/4 4 Pin, made in USA, buyultraviolet.com, USA) with an arc length 29.5 cm. The reactor's height was matched to the length of the UV lamp to maximize the effective use of the lamp's emitting surface. By aligning the lamp length with the reactor height, the system ensures maximize distribution of UV light along the entire reactor chamber by reducing shadow zone. For side and top view of small and large reactors with diameters of 20 cm and 50 cm see figure 8. which represents the short and long path length.

Small Reactor

a

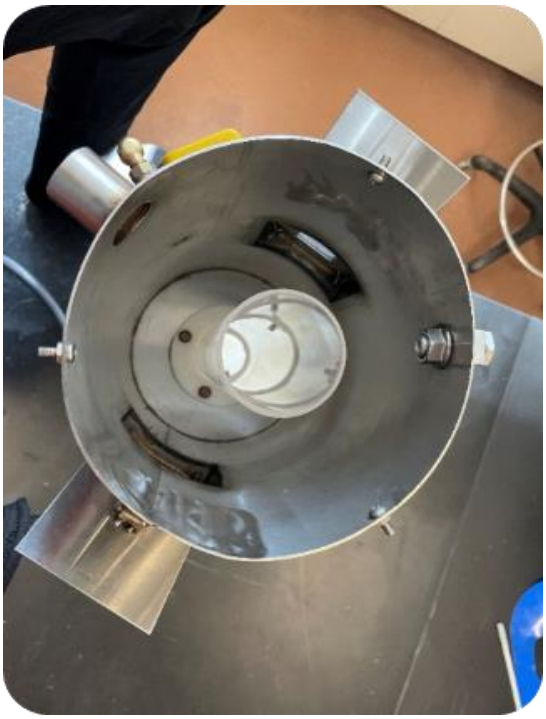

b

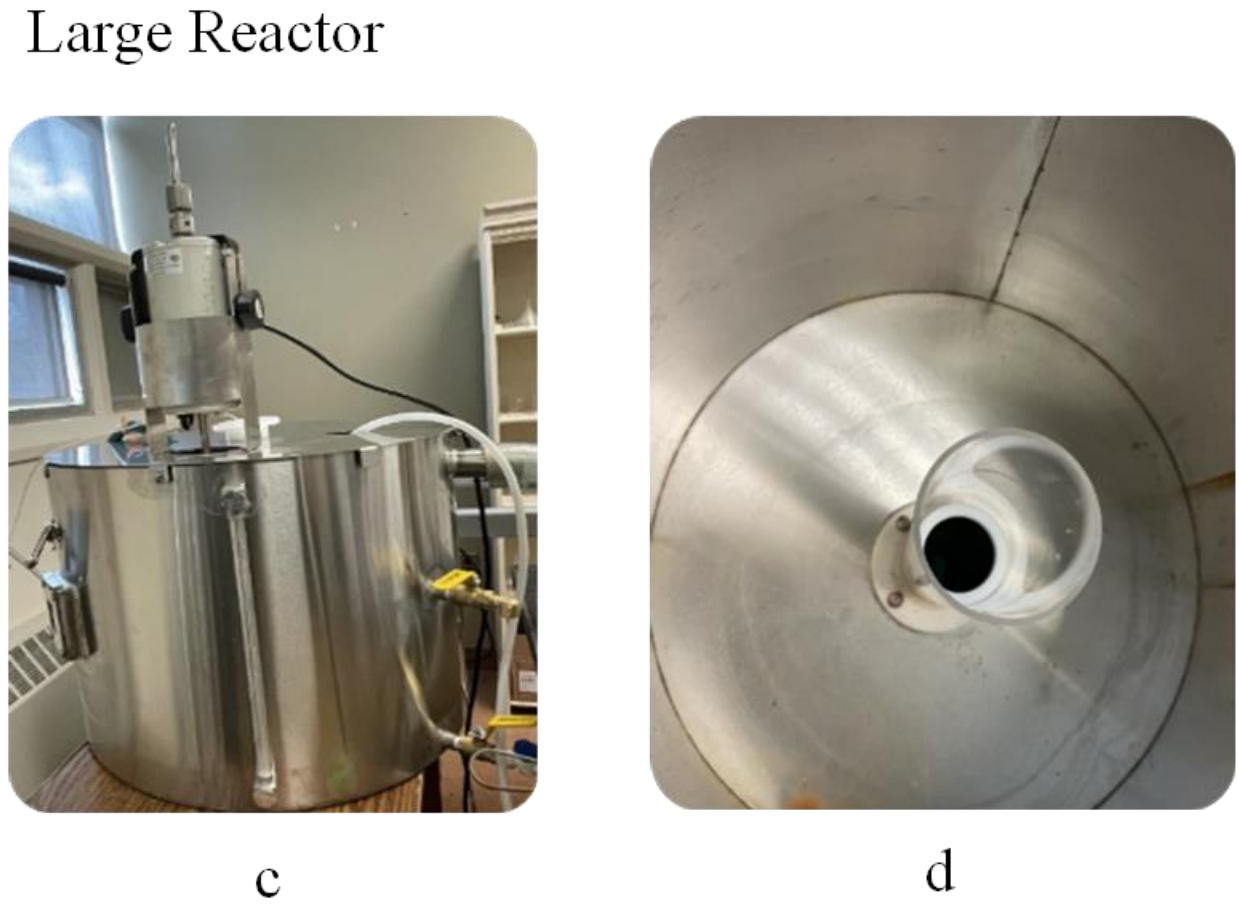

Figure 8. Representation of (a) side, (b) top view of small reactor d= 20 cm and (c) side, (d) top view of large reactor d= 50 cm for short and long path length

The reactor is made of stainless steel as most of UV reactors are made of this material. It also offers durability and corrosion resistance, making it suitable for long-term water treatment applications (Pan et al., 2025). The UV lamp is centrally positioned within the reactor, surrounded by quartz sleeve (d= 6 cm). The quartz prevents direct contact of water by the UV lamp. A mechanical mixer is positioned at the top of the reactor to ensure proper mixing of water and chemicals. It also promotes distribution of microbubbles. (Figure 9) shows the 3D view of reactor design showing the essential features of the reactor.

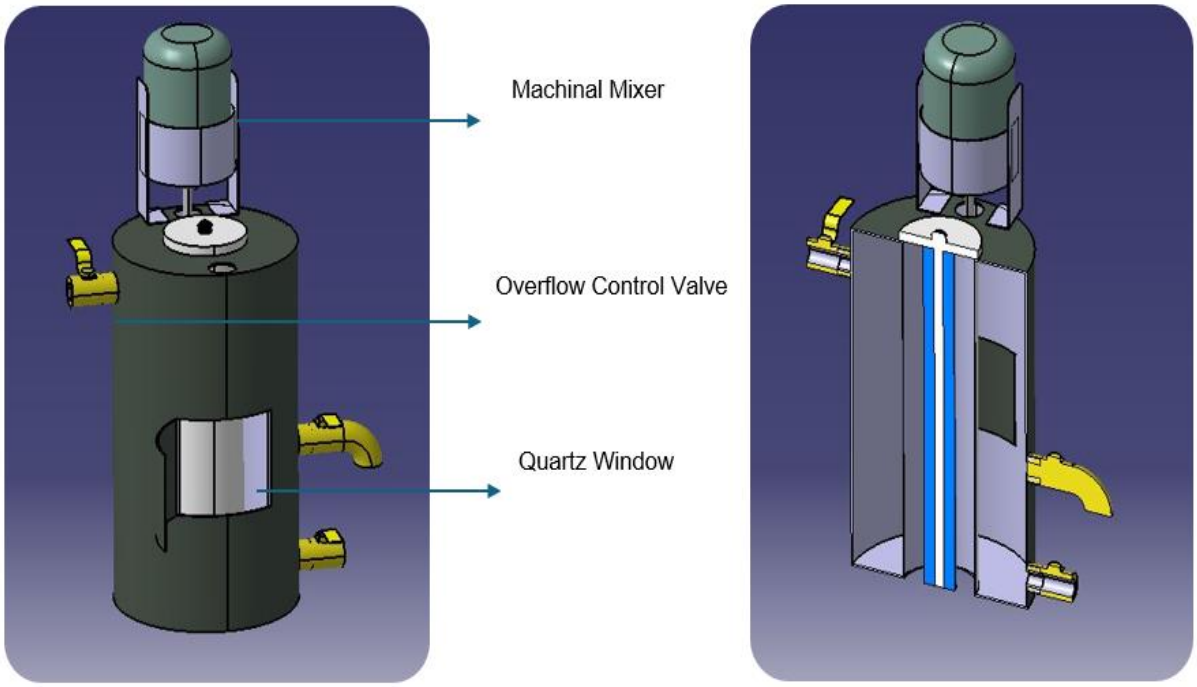

Figure 9. 3D view of the reactor design showing the essential features of the reactor.

Shutter Mechanism

Another feature of the reactor is the stainless-steel shutter mechanism located at the bottom. During the photochemical process, the shutter can push down to allow UV light to pass through the reactor, enabling the system to operate only when treatment is required. Instead of switching the UV lamp on and off, which can reduce lamp life, the shutter can be pushed up and down. This helps maintain consistent UV intensity, protects the lamp, and ensures the reactor is only exposed to UV during treatment.

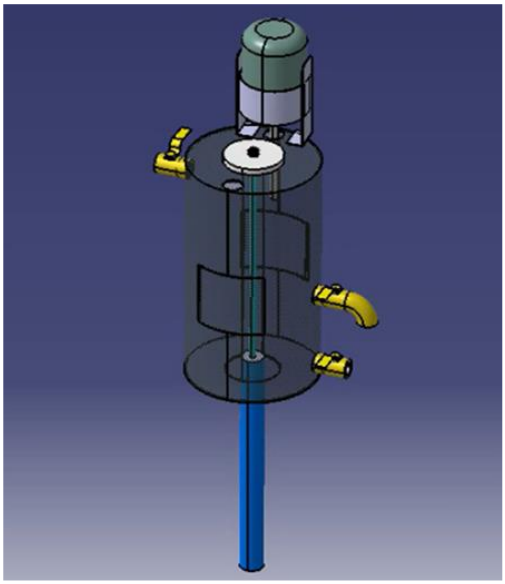

Figure 10. Working mechanism of a shutter in a 3D view.

3.2 Microbubble Generation

The experimental setup for microbubble generation, as shown in Fig 10, is consisted of a CARMIN diffuser D2 single-assembly microbubble generator (model D2-20-021, PMMA; YLEC Consultants, France) and a recirculation system. A recirculation pump (Model/ASIN: B0842KTN25, Duobang Fitness, China) was used to circulate water through the UV-AOP reactor and the diffuser unit with the flow rate (q) of 7 L/min. Within the diffuser, a spiral flow mechanism promoted air–water interaction, leading to the formation of microbubbles.

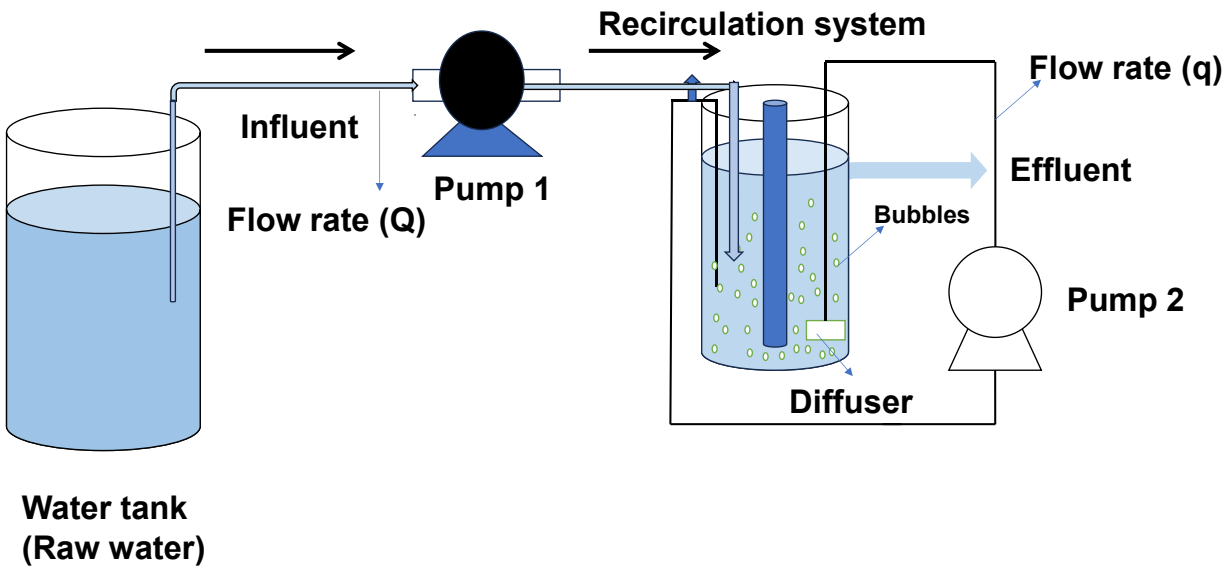

Figure 11. Process flow diagram for the generation of bubbles using recirculation system with the flow rate (q) in a continuous flow through reactor with tap water.

3.2.1 Method for Quantification of Microbubbles

Accurate measurement of bubble size and distribution was essential to evaluate the performance of microbubble generation and its potential influence on the UV-Advanced Oxidation Process. In this study, two independent techniques, microscopic observation and laser diffraction were used to determine the bubble size distribution and to cross-validate the results.

Bubble Size Distribution Analysis Using MasterSizer 3000

To analyse the size distribution of the generated microbubbles, a Malvern Panalytical Mastersizer 3000 (Malvern Panalytical Ltd., Malvern, Worcestershire, UK) was used, which operates on the laser diffraction principle. Two samples were prepared for this analysis: a blank sample containing only deionized (DI) water, and a second sample containing microbubbles generated under the same flow conditions. The bubbles were produced on-site in 1000 mL, and immediately after generation, 10 mL of the sample was transferred into the Mastersizer's

specialized measurement cell. No samples were stored for later use; each was analyzed immediately after collection to avoid changes in bubble size or concentration that can occur within minutes of storage.

Microscopic Analysis of Bubbles

In addition to laser diffraction, microscopic imaging was conducted to visually observe the bubbles and assess their size and shape. Microbubbles were generated in a 1000 mL beaker filled with DI water to avoid interference from pre-existing particles. Before initiating bubble generation, blank samples were run to ensure the accuracy and cleanliness of the system. A 3 mL sample of the bubble-containing water was carefully collected and transferred into a petri dish for observation under a light microscope. To obtain a representative image of the bubbles, three snapshots were taken from different areas of the petri dish. These images were then analyzed using ImageJ software to determine the size distribution and morphology of the microbubbles.

3.3 Method for Analysis of Free Chlorine and Hydrogen Peroxide Concentration

This section provides an overview of the experimental approaches used to quantify free chlorine and hydrogen peroxide, detailing the analytical techniques applied for each oxidant.

Chemicals

All reagents used in this study were of analytical or reagent grade to ensure experimental reliability and reproducibility. Deionized water (18.2 MΩ·cm) was produced using a Milli-Q purification system. The primary chemicals included sodium hypochlorite (NaOCl) solution (5.65–6 wt%, Fisher Chemical), hydrogen peroxide (H_2O_2) (30 wt%, Sigma-Aldrich), N,N-diethyl-p-phenylenediamine (DPD) indicator (Sigma-Aldrich), and disodium

ethylenediaminetetraacetate (Na_2EDTA) (Sigma-Aldrich). These chemicals were used as received without further purification. The experimental setup also incorporated a peristaltic recirculation pump, UV reactor chamber, LP and MP UV lamps, a mechanical overhead mixer, and a gas diffuser for microbubble generation. All instruments were routinely calibrated prior to use to ensure measurement accuracy and consistent operational performance.

Caffeine (ACS grade), benzoic acid (ACS grade), and nitrobenzene (ACS grade) were obtained from Sigma-Aldrich and used without further purification. Stock solutions of each compound were prepared using HPLC-grade water for calibration purposes and the required experimental concentrations were achieved by diluting this commercial solution into tap water, which served as the water matrix for all UV irradiation tests.

Standard solutions ranging from 1–25 μM were prepared in HPLC-grade water to establish calibration curves for the three micropollutants. Methanol (HPLC grade) was used for mobile phase preparation, while phosphoric acid (ACS grade) was used to adjust the aqueous mobile phase to pH 4, as required for chromatographic separation. Acetonitrile (HPLC grade, ≥99.9% purity) was used only for HPLC system cleaning and shutdown procedures and was not part of sample preparation or analysis

Analysis of Free Chlorine

Free chlorine concentration was measured using the N, N-diethyl-phenylenediamine (DPD) colorimetric method, following standard procedures recommended for drinking water analysis.

Free chlorine concentration was determined using Hach Method 8021 (DPD Method):

- The DR900 colorimeter was set to Program 80 (Free Chlorine, DPD Method).
- A 10 mL sample cell was rinsed and filled with the test sample.

- One DPD Free Chlorine Reagent Pillow was added and gently mixed for ≈ 30 s.
- The sample was immediately analyzed with the 'READ' function to record chlorine concentration.

Each sample was measured in duplicate, and the mean value was reported. All analyses were performed within one minute of reagent addition to prevent signal loss.

Analysis of Hydrogen Peroxide

The analysis of hydrogen peroxide (H_2O_2) at concentrations as low as 1 μM is performed by determining the yield of triiodide (I_3^-), which forms when H_2O_2 reacts with potassium iodide (KI) in a buffered solution containing ammonium molybdate as a catalyst. The absorbance of the resulting solution is measured at 351.0 nm (Frew et al., 1983).

Reagents and Equipment

Reagents:	
Potassium iodide (KI), ACS Grade	Spectrophotometer (set at 351 nm)
Sodium hydroxide (NaOH), ACS Grade	Analytical balance
Ammonium molybdate tetrahydrate, ACS Grade	Quartz cuvette (1 cm)
Potassium hydrogen phthalate (KHP), ACS Grade	Glass vials (25 mL)
Milli-Q water	

Procedure

Prepare solution A by dissolving 16.5 g KI, 0.5 g NaOH, and 0.05 g ammonium molybdate tetrahydrate in 250 mL Milli-Q water. Store in an amber bottle in the dark. Stir for approximately 10 minutes. Solution A should have a pH of 12.8. Solution B can be prepared by adding 5 g KHP in 250 mL Milli-Q water. Solution B should have a pH of 4.03. Mix equal weights of Solutions A and B. Add 2.5 mL of solution A and solution B in a 25 mL glass vial. Add the sample (H_2O_2) solution in varying volumes to achieve ~0.9 absorbance.

- For 10 mg/L: add 0.5 mL sample (total volume 5.5 mL)
- For 5 mg/L: add 1.5 mL sample (total volume 6.5 mL)
- For 1 mg/L: add 2.0 mL sample (total volume 7.0 mL)

Wait 1 minute, then measure absorbance at 351 nm in a 1-cm quartz cuvette. Determine blank absorbance: subtract Milli-Q water absorbance from that of the A/B mixture. Prepare blanks and zero readings for each dilution using Milli-Q water and sample water.

Calculate H_2O_2 concentration using the formula:

$$\frac{mg}{L} H_2O_2 = \frac{A_{351} \times \frac{Total\ Volume}{Sample\ Volume} \times 34 \frac{g}{mol} \times 1000 \frac{mg}{g}}{26450\ M^{-1}cm^{-1}}$$

Densities for Weight Measurements

- Solution A: 1.054 g/mL
- Solution B: 1.014 g/mL
- Equi-weight of A, B, and H_2O: 1.017 g/mL

- 10^{-3} M H_2O_2: 0.997 g/m

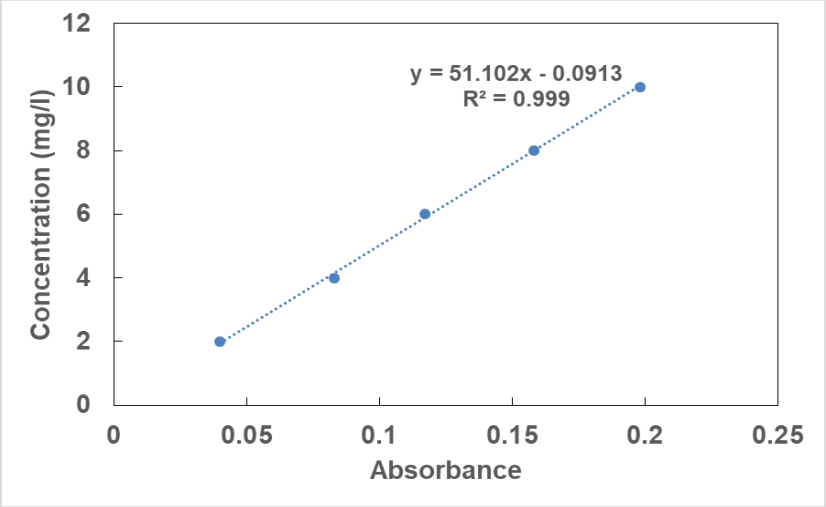

Figure 12. Calibration curve for hydrogen peroxide H_2O_2 with DI water using 1 cm cuvette for absorbance measurement.

3.4 Experimental Procedure for Oxidant Decay Monitoring

Experimental Procedure

The experimental setup employed in this study consists of a continuous flow-through UV reactor allows precise control over operational parameters (e.g., flow rate, reactor volume, lamp type etc.). The reactor comprises a cylindrical chamber, optimized to maximizing water residence time and UV light exposure. Two types of UV lamps were used within the reactor, low-pressure (LP) and medium-pressure (MP) lamps as each different in emission spectrum and photon flux which leads to major differences in oxidant photolysis, •OH generation, and micropollutant degradation. LP lamps emit almost entirely at 254 nm, while MP lamps emit a broad spectrum (200–400 nm) with much higher total power. Because different oxidants and pollutants absorb UV at different wavelengths, their reactions can behave very differently

under each lamp type. This lamp configuration allows for a comparative assessment of their performance individually under different experimental conditions.

As shown in Figure 4.4.2, raw water spiked with H_2O_2 or chlorine was stored in a water tank, which was pumped continuously to the UV reactor at designed flow rates, using a pump a with flow rate range of 1-20 L/min (Model: MEDAS 330 GPH 115V 1/10 HP, Manufacturer: MEDAS, China). In the UV reactor, bubbles were introduced through the diffuser. At a fixed flow rate and a constant bubble generation rate, a steady state of oxidant concentration, bubble concentration, and pollutant concentration were maintained in the UV reactor. To prevent hydraulic short-circuiting and promote uniform contact between water and reactants, the inlet and outlet ports were positioned at different vertical levels. At the top of the reactor, a mechanical mixer was installed to maintain homogeneous mixing and facilitate even distribution of microbubbles within the reactor volume. This configuration enabled the reactor to achieve consistent microbubble dispersion and stable operating conditions for all experimental trials.

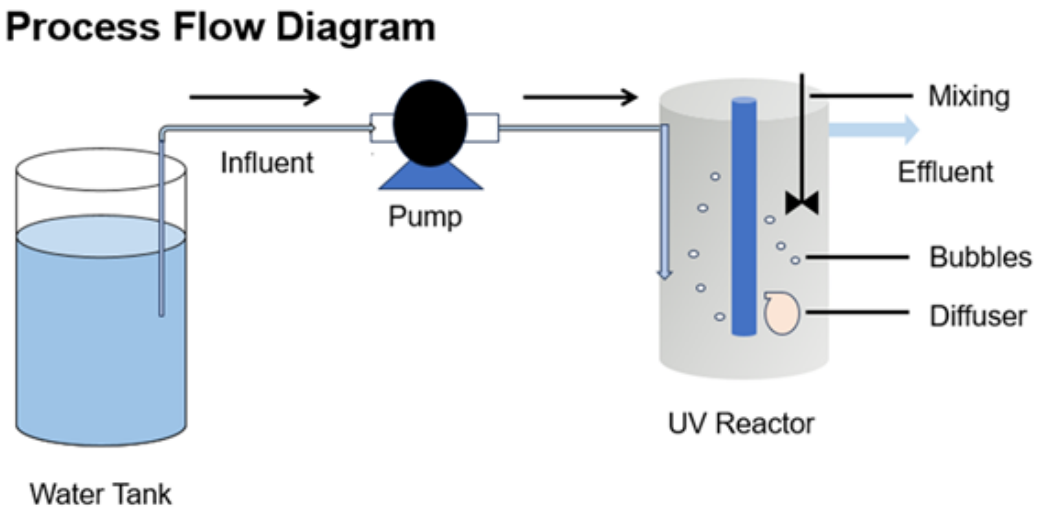

Figure 13. Process flow diagram for oxidant decay analysis using tap water as source water.

Monitoring the Decay of Oxidants

The ultimate objective of this study is to enhance the removal of micropollutants through Advanced Oxidation Processes (AOPs). It is hypothesized that introducing air bubbles, particularly microbubbles, can enhance the degradation efficiency by improving photon utilization within the UV reactor. This initial stage focuses on establishing a proof of concept through oxidant decay monitoring. In this experiment, the bubble concentration inside the UV reactor was controlled by adjusting the water flow rate. The diffuser continuously generates a uniform stream of microbubbles at a fixed rate, so the only variable affecting bubble density is the hydraulic flow (Q). At lower flow rates, the water moves more slowly, allowing bubbles to accumulate and resulting in a higher bubble concentration. In contrast, increasing the flow rate dilutes the bubbles more effectively and reduces their overall concentration in the reactor. By using different flow rates, the system can achieve distinct bubble concentrations while keeping the bubble generation rate constant. The decay of oxidants (e.g., H_2O_2 in UV/H_2O_2 or Cl_2 in UV/Cl_2 systems) is used as an indirect indicator of photon utilization. The oxidant decay rate is closely correlated with the rate at which photons are absorbed and utilized to generate reactive radicals. Therefore, if aeration enhances photon utilization within the reactor, it should result in a higher oxidant decay rate.

Two experimental conditions are tested:

- Without aeration (controlled condition): Water flows through the reactor without bubble injection.
- With aeration: bubbles are introduced to the reactor using a diffuser.

The oxidant decay rate (k) is determined assuming first-order kinetics, using the relation:

$$k = \frac{-\ln\left(\frac{C_T}{C_O}\right)}{t}$$

k is the decay rate constant.C_0 and C_T are the initial and final oxidant concentrations respectively, and t is the hydraulic retention time calculated as

$$t = \frac{V}{Q}$$

in which V is the volume of the reactor, and Q is the flow rate.

Therefore, if our hypothesis holds true, the oxidant decay rate under aerated conditions (k_{air}) should be higher than under non-aerated conditions ($k_{no\text{-}air}$), resulting in a ratio greater than 1. This outcome would indicate that bubbles enhance photon utilization, which in turn is expected to improve micropollutant degradation in subsequent studies.

The performance enhancement due to aeration can be evaluated through the ratio:

$k_{air}/k_{no\text{-}air}$

- If $k_{air}/k_{no\text{-}air} > 1$: Aeration enhances photon utilization, leading to faster oxidant decay
- If $k_{air}/k_{no\text{-}air} = 1$: Aeration has no observable effect.
- If $k_{air}/k_{no\text{-}air} < 1$: Aeration negatively affects photon transmission, possibly due to excessive bubble density reducing light penetration near the UV lamp surface.

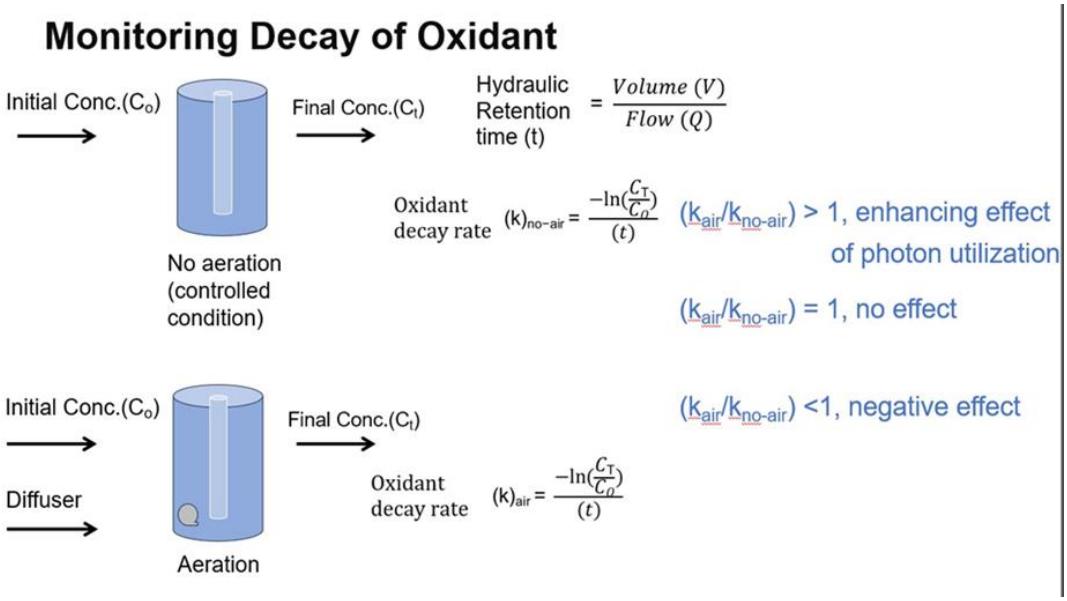

Figure 14. Monitoring Decay of Oxidant

3.5 Analytical Methods for Micropollutants decay analysis

Analytical Methods

HPLC Analysis of Micropollutants

The concentrations of caffeine, nitrobenzene, and benzoic acid were determined using a High-Performance Liquid Chromatography (HPLC) system equipped with a diode-array detector (DAD). Chromatographic separation was conducted using a C18 reversed-phase column. The mobile phase consisted of:

- Mobile Phase A: methanol
- Mobile Phase B: 10% methanol in deionized water, adjusted to pH 4 using phosphoric acid

A gradient program was employed, beginning with 30% A and 70% B, increasing to 70% A and 30% B, and then returning to the initial conditions. This gradient provided clear separation

and consistent detection of all three compounds. Sample collected from the reactor were passed through a 0.2 μm membrane filter prior to injection to remove particulate matter and protect the HPLC column. Each micropollutant was identified based on its retention time during HPLC analysis: caffeine at 5.27 min, benzoic acid at 10.05 min, and nitrobenzene at 10.83 min. The method also provided low detection limits, measured at 0.15 μM for caffeine, 0.1 μM for benzoic acid, and 0.14 μM for nitrobenzene, ensuring accurate quantification throughout the experiments.

Quality Assurance

All HPLC analyses were performed in duplicate. Calibration curves for caffeine, benzoic acid, and nitrobenzene were generated at the start of each analytical session to determine the association between the concentration of the sample and the peak area. DI water blanks were routinely injected to confirm the absence of background contamination. Solvent blanks and instrument blanks were used as needed to verify system cleanliness, check for carryover, and ensure stable baselines. All samples were filtered (0.2 μm) immediately prior to analysis to maintain column performance and analytical consistency.

3.6 Results and Discussion

This section brings together the complete set of experimental findings that support the evaluation of the microbubble-assisted UV-AOP system used in this study. First, the characteristics of the generated microbubbles are presented, based on particle-size measurements from the Mastersizer 3000 and microscopic image analysis, to establish the size distribution and stability of the bubbles within the reactor. The second part examines the decay of the added oxidants under aerated and non-aerated conditions, which serves as a proof-of-concept for how microbubbles affect radical generation. Finally, the third section reports the

degradation performance of the selected micropollutants caffeine, benzoic acid, and nitrobenzene allowing direct study of enhanced micropollutant removal through aeration. Together, these results offer a coherent picture of how microbubble introduction shapes both the chemical and physical processes governing pollutant removal in the system.

3.6.1 Microbubbles Size Analysis (Microscopic Observation and Laser Diffraction)

A detailed evaluation of the microbubble size distribution was carried out using both microscopic imaging and laser diffraction. From the microscopic analysis, it was observed that the CARMIN diffuser produced fine, stable microbubbles that were predominantly within the targeted range of 10 to 100 micrometers. The bubbles appeared well-dispersed, nearly spherical in shape, and showed minimal coalescence during the observation period. The average diameter determined from the microscopic images was approximately 80 µm, indicating consistent and controlled bubble formation throughout the experiments. See figure 13. represents average bubble size with microscopic analysis using CARMIN diffuser.

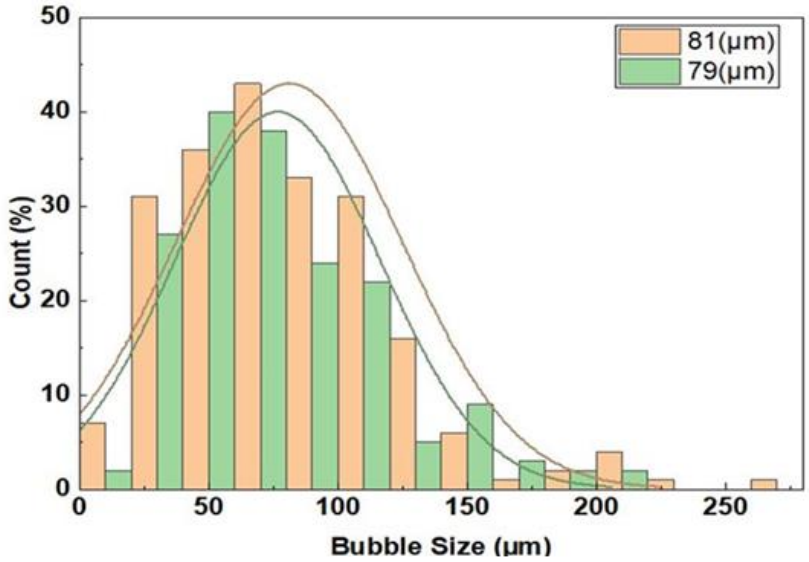

Figure 15. Average bubble size with microscopic analysis, bubbles generated by CARMIN diffuser using tap water.

To validate these results, laser diffraction measurements were performed using the Malvern MasterSizer 3000. The results showed a mean bubble diameter (D_{50}) of about 77 µm, which closely matched the value obtained from microscopy. The size distribution curve obtained from the MasterSizer showed a single dominant peak, confirming that the generated microbubbles were uniform and fell within a narrow range. The strong agreement between these two independent methods supports the accuracy and repeatability of the measurements and demonstrates the reliability of the CARMIN diffuser in producing microbubbles with stable and consistent characteristics.

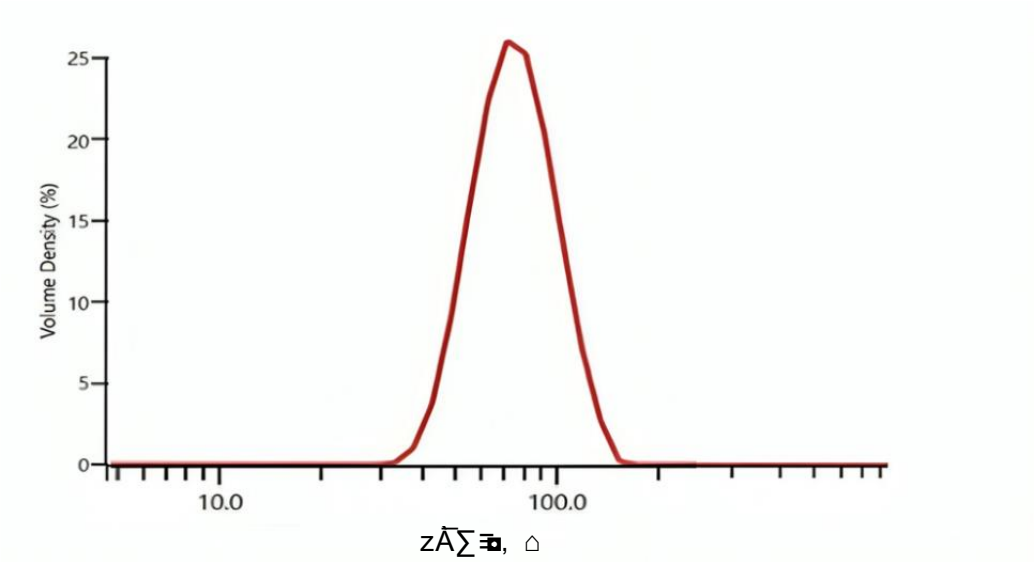

Figure 16.Bubble size distribution curve by Mastersizer 3000 by CARMIN diffuser using tab water at room temperature.

These observations are consistent with previous findings reported in the literature (Couto et al., 2009; Lee et al., 2019), where microbubbles in the range of 10 – 100 µm were shown to improve light distribution and mass transfer in photochemical systems. Therefore, the close match between microscopic and laser diffraction results not only confirm the precision of the

measurement techniques but also highlights that the diffuser successfully generates microbubbles of size range for efficient UV-AOP performance.

3.6.2 Oxidant Decay Rate

This section presents the results of oxidant decay under varying flow rates (Q) and aeration conditions in both small and large UV reactors. The study evaluates how bubble-induced scattering and reflection influence photon path length, retention time and overall photon utilization efficiency. The discussion also compares the behavior of two oxidants chlorine (Cl_2) and hydrogen peroxide (H_2O_2) with different flowrates, bubbles concentration, different reactor sizes and under low-pressure (254 nm) and medium-pressure UV lamps.

Effect of Flowrate and Bubble Concentration

The flowrate (Q) was used as an indirect control for bubble concentration inside the continuous-flow UV reactor. Since the diffuser supplied constant stream of bubbles, reducing the hydraulic flowrate (Q) increased bubble concentration, while higher water flowrates reduced the number of bubbles in the reactor. At low flowrates, the bubble concentration was high, making light (photons) not able to escape from the surface of UV lamp leading to a condition where they cannot effectively penetrate the bulk water, resulting in a ratio less than 1, a clear negative aeration effect. As the flowrate increased, bubble concentration became more balanced, improving photon distribution through scattering and reflection. At a flow rate of around 13 L/min, which was identified as optimal flowrate, the bubble concentration reached an ideal level. This resulted in the $k_{air}/k_{no\text{-}air}$ ratio peaking at approximately 2.6 for Cl_2 and 2.1 for H_2O_2 in a small reactor, as illustrated in Figures 18 & 19 under the low-pressure UV lamp.

(a)

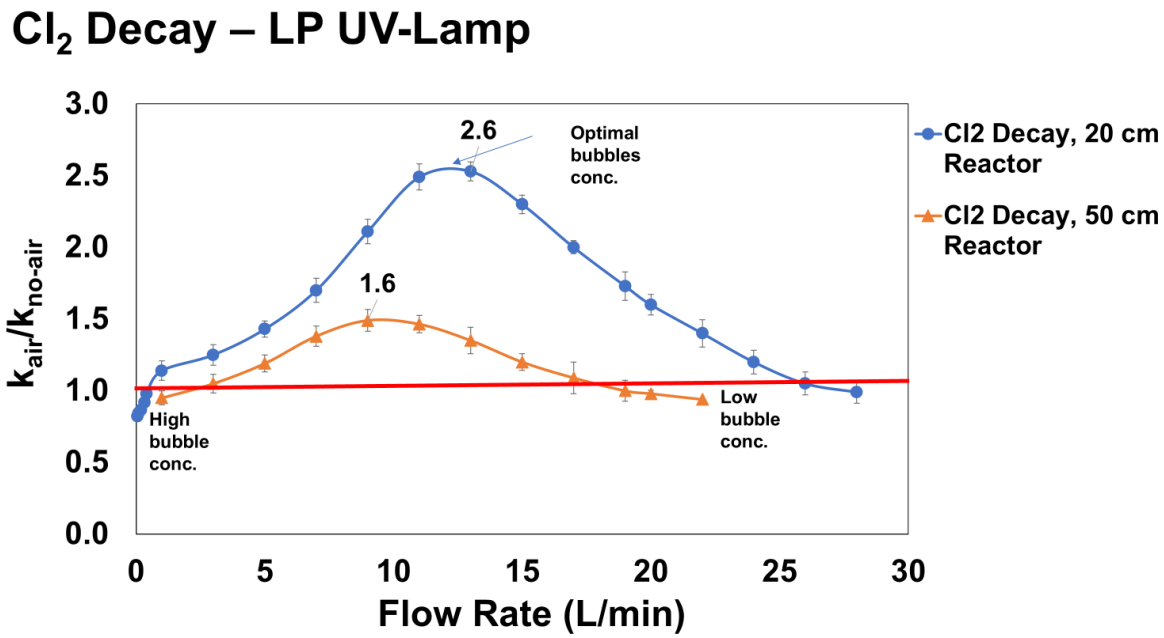

Figure 17 Ratio of Cl_2 decay curves in small and large reactors with 10 mg/L concentration, with and without aeration using low pressure UV lamp.

This demonstrates that under these conditions, the oxidant decay rates peaked at about 2.6 and 2.1 times higher with aeration than without, confirming a significant enhancement in photon utilization within the reactor. Beyond this optimal point, further increases in flowrate decreased the concentration of bubbles to a level where scattering effects diminished and photons once again passed through the water with minimal reflection or scattering, causing the ratio to return close to unity.

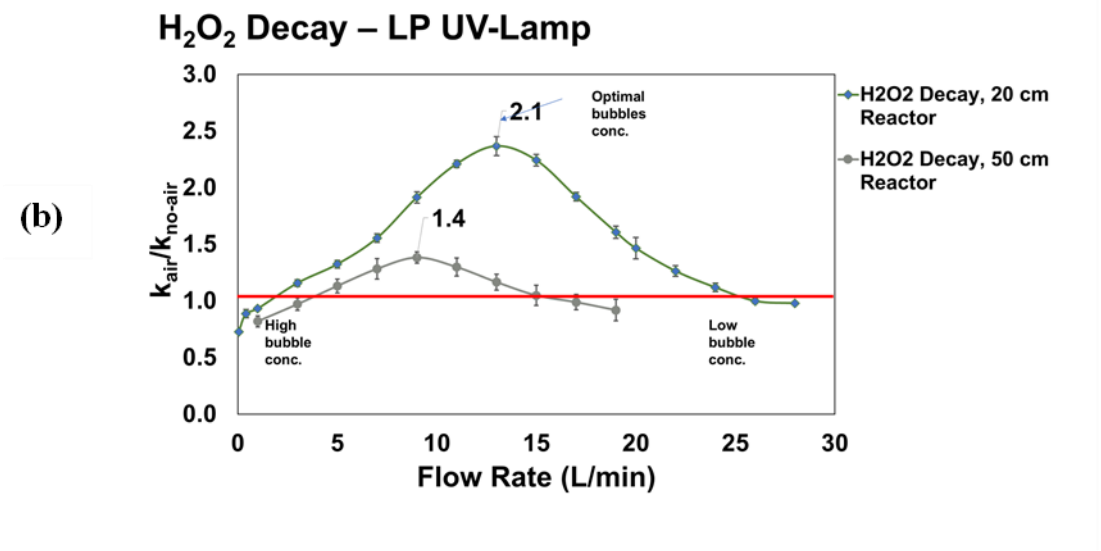

Figure 18 Ratio of H_2O_2 decay curves in small and large reactors with 10 mg/L concentration, with and without aeration using low pressure UV lamp.

Overall, this behavior reflects a balance between photon scattering and photon transmission:

- At low flowrate (too many bubbles) → photon blockage and poor light penetration.
- At moderate flowrate (optimal bubbles) → improved photon utilization and enhanced reaction rate.
- At high flowrate (too few bubbles) → reduced scattering and increased photon loss to the reactor wall.

This trend shows that microbubble-assisted UV reactors must be optimized for bubble concentration.

Effect of Rector Sizes

The influence of reactor size was also evident. The small reactor (20 cm) exhibited a higher peak ratio compared to the large reactor (50 cm), even though both followed the same overall

pattern (rise, peak, decline). In the small reactor, photons travel a shorter distance before reaching the reactor walls, which leads to greater photon losses under non-aerated conditions. This means that there is more room for improvement of photon efficiency in the small reactor than in the large reactor. Introducing bubbles will scatter and reflect photons back into the bulk solution, achieving such improvement of photon efficiency. This is why the $k_{air}/ k_{no\text{-}air}$ ratio is higher in the small reactor, reaching approximately 2.6 for chlorine and 2.1 for hydrogen peroxide respectively.

In contrast, in the large reactor, photons have a longer path length and a higher probability of interacting with oxidants before being absorbed or reflected. As a result, the baseline photon utilization is already higher, and the relative benefit of aeration is smaller. While the same scattering and reflection mechanisms operate in both reactors, their impact is more pronounced in smaller systems where photon losses are initially dominant. Accordingly, the improvement in photon utilization through aeration is less significant in the large reactor, with the ratio reaching approximately 1.6 for chlorine and 1.4 for hydrogen peroxide.

Oxidant Decay Under Medium Pressure UV Lamp

Under medium-pressure UV (MPUV) irradiation, which emits a broad spectrum between 200–400 nm, a significant enhancement in oxidant decay was observed for both chlorine and hydrogen peroxide in the aerated conditions compared to the non-aerated ones. The ratio $k_{air}/k_{no\text{-}air}$ followed a consistent trend across both reactor sizes and oxidants: it initially increased with flow rate, reached an optimum condition, and then declined. The ratio peaked at approximately (3.1&2.7) for chlorine and (1.9&1.7) for hydrogen peroxide in the small (20 cm) and large reactors respectively, indicating optimal bubble concentration and maximum enhancement of the photon utilization rate. Reactor geometry also played a crucial role: in the small reactor, photons had a shorter path length and were more likely to reach the wall and be

lost under non-aerated conditions, making the scattering and reflection from bubbles far more beneficial. In contrast, the large reactor (50 cm) already provided a longer optical path and better baseline photon distribution, resulting in a lower but still noticeable enhancement (1.9 for chlorine and 1.7 for hydrogen peroxide) as illustrated in Figure 21.

(c)

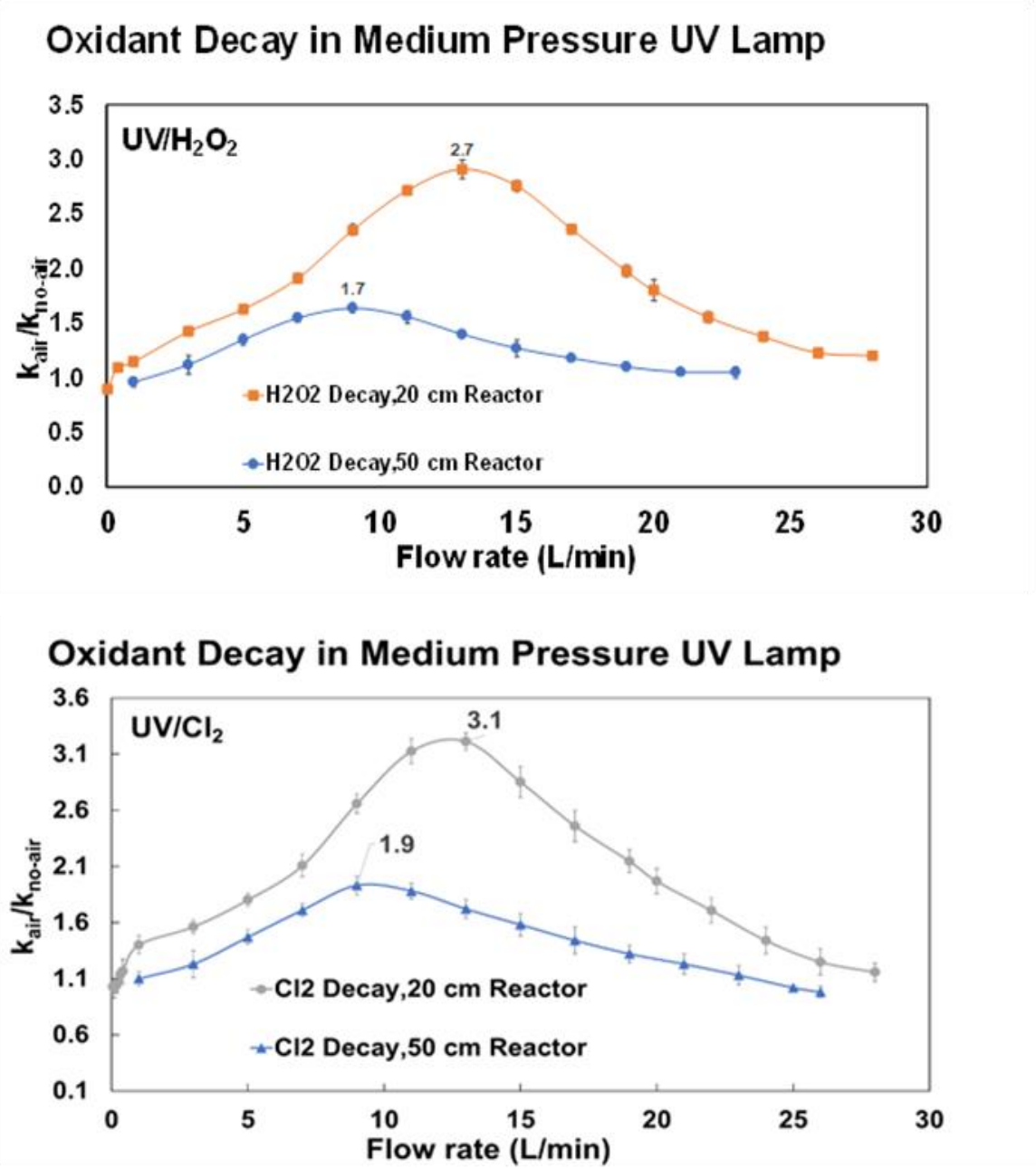

Figure 19. Decay curves of Cl_2 and H_2O_2 for small & large reactors under medium pressure UV lamp system.

This stronger performance of the MPUV system can be attributed to its broader emission spectrum. Unlike LPUV, which primarily emits at 254 nm, the MPUV lamp provides a continuous range of wavelengths, including longer ones that can penetrate deeper into the reactor. These longer wavelengths have higher transmittance, allowing photons to travel farther as a result, more photons reach the reactor walls and be wasted so there is more potential to enhance photon utilization rate. Consequently, MPUV irradiation achieves higher oxidant decay peaks and overall photon utilization compared to LPUV systems.

3.6.3 Micropollutant Decay

The third stage of this study focuses on the degradation of a ternary mixture of caffeine, benzoic acid, and nitrobenzene under two widely used UV-based advanced oxidation processes: UV/H_2O_2 and UV/Cl_2. All experiments were conducted in the 20-cm reactor, operated at the optimal hydraulic condition of 13 L/min, previously determined based on oxidant decay analysis (Section 3.6.2). Micropollutants were spiked at 20 μM each into tap water, and experiments were performed with and without aeration, using the CARMIN microbubble diffuser under identical settings as the oxidant-decay analysis. The enhancement ratio, k_{air}/k_{no-air}, was used to quantify the improvement produced by microbubble injection. A ratio greater than 1 indicates enhanced photon utilization due to bubble-induced scattering, reflection, and increased optical pathlength.

The results showed that microbubble injection consistently enhanced degradation across all conditions, but the degree of improvement depended strongly on oxidant dose, AOP type, and intrinsic micropollutant reactivity toward radicals. Caffeine, which reacts rapidly with both hydroxyl radicals ($k(\bullet OH) \approx 5.9 \times 10^9\ M^{-1}s^{-1}$) and chlorine radicals ($k(Cl\bullet) \approx 3–5 \times 10^9\ M^{-1}s^{-1}$), consistently showed the largest enhancement (Sun et al., 2016). Benzoic acid exhibits similar reactivity toward •OH ($\approx 5.9 \times 10^9\ M^{-1}s^{-1}$) but only moderate reactivity with chlorine radicals

(≈ 1–2 × 10^9 $M^{-1}s^{-1}$). Nitrobenzene, the most resistant compound in this mixture, reacts more slowly with both hydroxyl radicals (≈ 3.9 × 10^9 $M^{-1}s^{-1}$) and chlorine radicals (< 1 × 10^9 $M^{-1}s^{-1}$), explaining its generally lower but still consistent enhancement trends (Chae et al., 2023).

Micropollutant Degradation Under UV/Cl_2

At the lower chlorine dose (5 mg/L), aeration produced a pronounced enhancement of micropollutant degradation. The $k_{air}/k_{no\text{-}air}$ ratios were on the order of 2.4–2.6 for all three compounds, indicating that the presence of microbubbles approximately doubled to nearly tripled the pseudo–first-order decay constants relative to the non-aerated control. Caffeine showed the largest enhancement ($k_{air}/k_{no\text{-}air}$ ~2.6), while benzoic acid and nitrobenzene exhibited slightly lower, but comparable, values (2.4–2.5). These results demonstrate that under conditions where photon supply is limited (moderate oxidant dose, short optical path length), microbubble injection substantially improves the utilization of UV photons for micropollutant degradation. This behavior mirrors the oxidant-decay results in the same reactor, where aeration increased the chlorine decay rate by a factor of ~2.6 at the optimal flowrate.

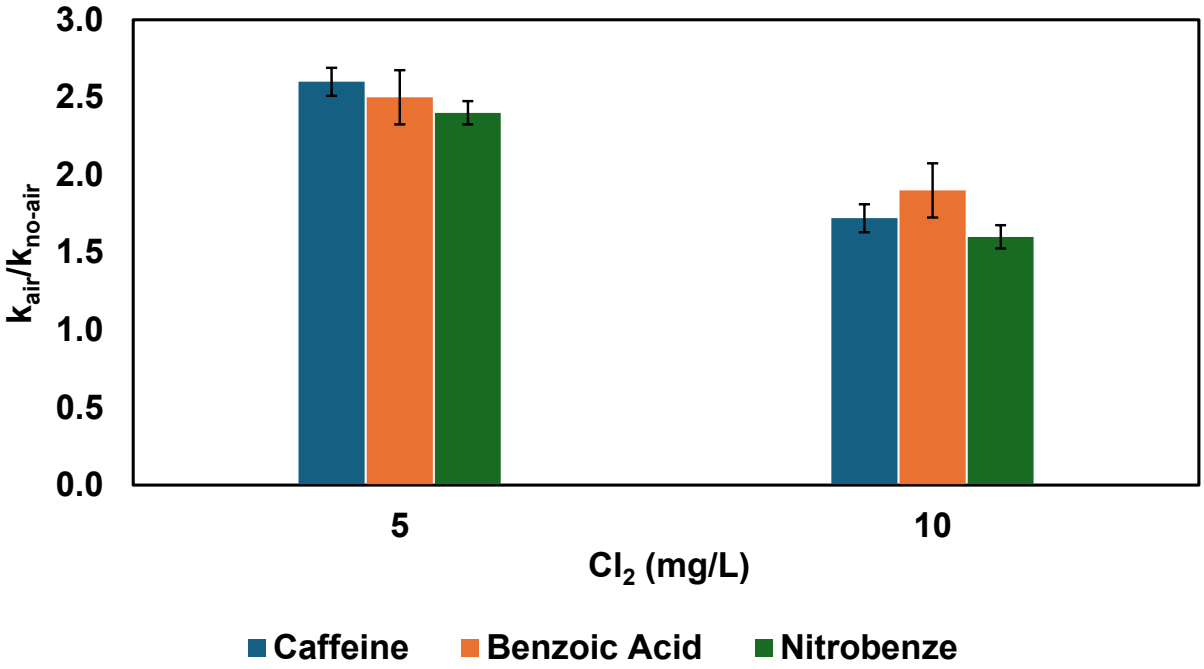

Figure 20 Enhancement ratio (k_{air}/k_{no-air}) for caffeine, benzoic acid and nitrobenzene under UV/Cl_2 at 5 and 10 mg/L in the 20 cm reactor (tap water matrix, 13 L/min; initial concentration 20 µM each).

The close agreement between oxidant and micropollutant enhancement factors suggest that the improved decay of chlorine under aerated conditions indeed translates into more efficient radical production and, ultimately, faster destruction of organic contaminants.

When the chlorine dose was increased to 10 mg/L, the enhancement ratios decreased to 1.5–1.7. Although aeration still improved degradation, the effect was smaller due to reduced photon limitation as at high concentration most photons are used by chlorine. Even so, caffeine continued to show the fastest improvement due to its high radical reactivity, while nitrobenzene, with slower reaction kinetics, showed slightly lower enhancement despite still benefiting from microbubble scattering.

Micropollutant Decay Under UV/ H_2O_2

The behavior of the UV/H_2O_2 system followed the same general pattern but with slightly lower enhancement values overall, reflecting the weaker absorption of H_2O_2 at 254 nm. At 5 mg/L H_2O_2, enhancement ratios ranged from 2.1 to 2.3, with caffeine again displaying the highest improvement (~2.3), followed by benzoic acid and nitrobenzene. These differences match their known hydroxyl radical reactivity: caffeine and benzoic acid possess nearly identical rate constants with •OH (~6 × 10^9 $M^{-1}s^{-1}$), whereas nitrobenzene reacts more slowly (~4 × 10^9 $M^{-1}s^{-1}$), leading to slightly reduced enhancement under the same photolytic conditions (Chae et al., 2023; Sun et al., 2016).

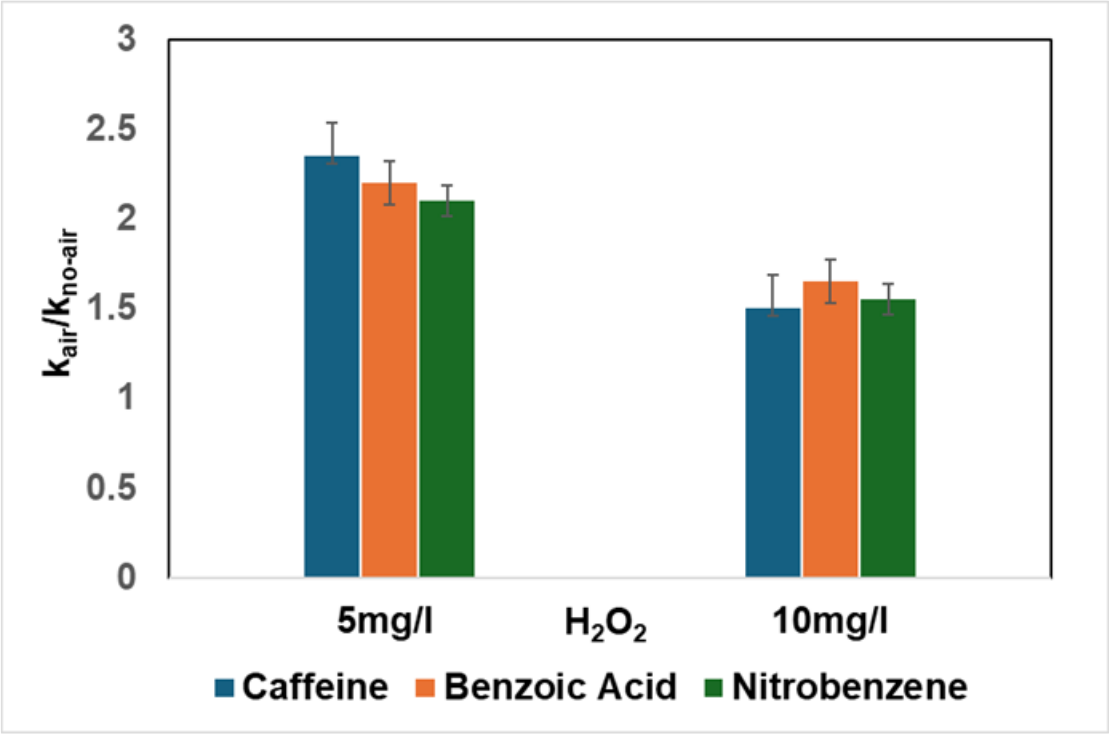

Figure 21 Enhancement ratio (k_{air}/k_{no-air}) for caffeine, benzoic acid and nitrobenzene under UV/H_2O_2 at 5 and 10 mg/L in the 20-cm reactor (tap water matrix, 13 L/min, initial concentration 20 µM each)

At the higher peroxide dose (10 mg/L), enhancement ratios dropped to 1.5–1.7, like the chlorine system. The decline is attributed to increased hydroxyl-radical scavenging by excess H_2O_2 and the reduced importance of photon limitation at higher oxidant levels. Even under these conditions, the relative reactivity of the micropollutants remained evident: caffeine consistently benefited the most, while nitrobenzene, being more resistant to •OH attack, showed the lowest gains.

Comparison between UV/H_2O_2 and UV/Cl_2 micropollutant degradation for different oxidant dosages (5 – 10 mg/L)

A comparison of the two AOPs revealed that at low oxidant dose, UV/Cl_2 and UV/H_2O_2 provides greater enhancement than high dosages of 10 mg/L. This is expected due to the lower photon absorption by oxidants (chemical) hydrogen peroxide and chlorine, and wastage is high with the walls of reactor. So, bubbles show greater enhancing effect at low dosages for the AOPs-system. However, at the higher oxidant dose of 10 mg/L, the enhancement ratios for both systems decreased relative to their low-dose performance. Both UV/Cl_2 and UV/H_2O_2 showed a similar trend of reduced enhancement at 10 mg/L, suggesting that high oxidant concentrations may introduce radical scavenging or shift the system closer to a photon-saturated regime, thereby diminishing the relative benefit of aeration in both AOPs.

Importantly, the micropollutant degradation patterns closely mirrored those observed during oxidant-decay testing. Enhancement peaked at moderate oxidant concentrations, decreased at higher doses. This strong alignment demonstrates that oxidant-decay enhancement (k_{air}/k_{no-air}) is a reliable surrogate for predicting micropollutant degradation performance. Practically, this means that rapid oxidant-decay tests can be used to pre-screen reactor conditions before undertaking more complex micropollutant experiments, significantly reducing experimental time and cost.

Degradation of Micropollutants Under Medium Pressure UV lamp

UV/Cl_2 System at Medium Pressure

The MP UV/Cl_2 system continued to show strong benefits from aeration, particularly at the lower oxidant concentration. At 5 mg/L chlorine, enhancement ratios increased noticeably for all three compounds, with average values of approximately:

- Caffeine: ~2.85
- Benzoic acid: ~2.55
- Nitrobenzene: ~2.75

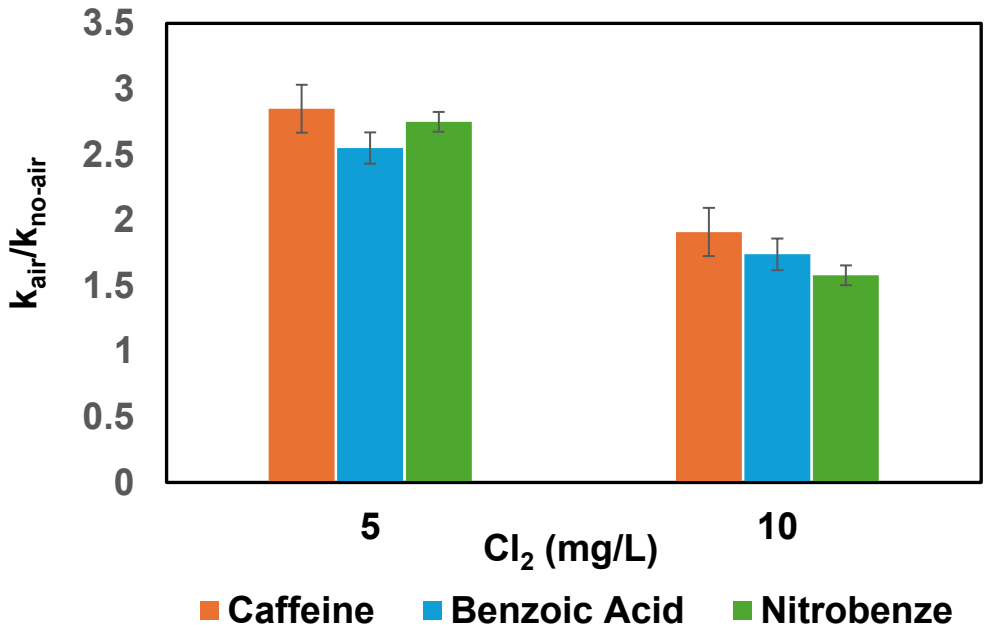

Figure 22 Enhancement ratio (k_{air}/k_{no-air}) for caffeine, benzoic acid, and nitrobenzene under medium-pressure UV irradiation with 5 mg/L and 10 mg/L chlorine in in the 20-cm reactor (tap water matrix, 13 L/min, initial concentration 20 µM each)

At the higher chlorine dose (10 mg/L), enhancement ratios decreased, ranging from: Caffeine: ~2.0, benzoic acid: ~1.8, nitrobenzene: ~1.6. Despite the reduction, values remained well above 1, demonstrating that aeration still provided meaningful benefits even when the system became

less photon limited. The reduced enhancement at 10 mg/L consists of increased absorption of photons by high concentration of chlorine, less photons will be wasted so the overall ratio of micropollutants decay is lower as compared to low concentration.

Medium Pressure UV/H_2O_2 System

The medium-pressure (MP) UV/H_2O_2 system displayed degradation trends consistent with those observed under MP UV/Cl_2, reaffirming the strong influence of microbubble-enhanced aeration on photon delivery and radical formation within the reactor. At the lower oxidant dose of 5 mg/L H_2O_2, the system showed comparatively high enhancement ratios for all three micropollutants. Caffeine and benzoic acid demonstrated enhancement ratios of approximately 2.55 and 2.30, respectively, while nitrobenzene reached a slightly higher value of ~2.70. This elevated response from nitrobenzene is expected due to its weaker direct UV absorbance and its stronger reliance on hydroxyl radical (•OH)-mediated pathways. In MP UV systems, where a broader wavelength spectrum is available, nitrobenzene benefits more from increased •OH production and improved photon utilization facilitated by aeration.

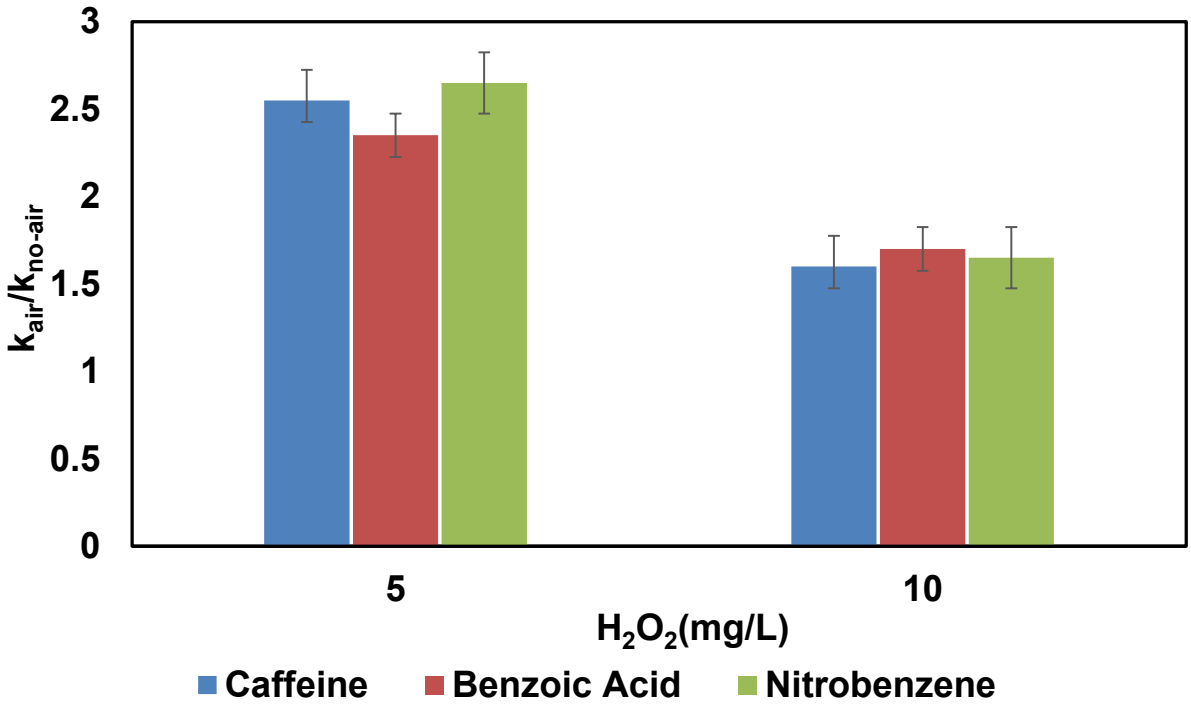

Figure 23 Enhancement ratio (k_{air}/k_{no-air}) for caffeine, benzoic acid, and nitrobenzene under medium-pressure UV irradiation with 5 mg/L and 10 mg/L hydrogen peroxide

When the oxidant dose increased to 10 mg/L H_2O_2, the enhancement ratios decreased across all pollutants, falling to values between 1.55 and 1.65. This reduction mirrors the behavior seen in the MP UV/Cl_2 system and indicates a transition away from photon-limited conditions. At higher peroxide concentrations, excess H_2O_2 begins to act as a photon competitor, increasing internal light screening and reducing the marginal benefit of improved photon transport provided by aeration. Additionally, radical scavenging by excess peroxide (H_2O_2 + •OH → HO_2• + H_2O) becomes more pronounced, further diminishing the relative enhancement provided by microbubble mixing.

Microbubble aeration has a greater positive impact on medium-pressure UV systems because MP lamps produce longer wavelengths that are vulnerable to wall losses. Microbubbles scatter these photons back into the reactor, improving photon utilization and increasing k_{air}/k_{no-air} more than in LP systems.

Conclusion

The results of this study show that the improvement in micropollutant removal observed with microbubble aeration is mainly driven by better use of UV photons inside the reactor. This conclusion is strongly supported by the clear and consistent relationship between oxidant decay and micropollutant degradation observed throughout the experiments. In both UV/H_2O_2 and UV/Cl_2 systems, conditions that produced faster oxidant decay under aeration also led to proportionally higher micropollutant removal. This close agreement confirms that oxidant decay can be used as a direct indicator of enhanced radical generation and overall treatment performance. Under moderate oxidant doses, where photon availability limits the process, microbubble aeration significantly improved reactor performance. The introduction of microbubbles increased the effective optical path length by scattering and redirecting UV photons back into the water instead of allowing them to be lost to the reactor walls. As a result, more photons were available to interact with oxidants, accelerating oxidant decay and increasing radical production. Because micropollutant degradation closely followed the same trend as oxidant decay, the results clearly indicate that the observed enhancement originates from improved photon utilization rather than from compound-specific effects.

At higher oxidant concentrations, the relative benefit of aeration became smaller, even though overall degradation remained high. This behavior reflects a shift away from photon-limited conditions. When excess oxidant is present, a large fraction of UV photons is already absorbed close to the lamp surface, leaving fewer photons available to benefit from redistribution by microbubbles. In addition, higher oxidant concentrations increase radical scavenging and internal light screening, which further reduces the marginal impact of aeration. The reduction in enhancement at higher oxidant doses therefore supports the proposed mechanism and helps define the operational range in which microbubble aeration is most effectivestronger response

observed in medium-pressure UV systems further reinforces the role of reactor optics in controlling performance. Medium-pressure lamps emit a broader spectrum of UV radiation that is more susceptible to wall losses in conventional reactors. Microbubble aeration was particularly effective under these conditions, as it redistributed polychromatic UV light and increased photon residence time within the reactor. This resulted in consistently higher enhancement ratios compared to low-pressure systems and highlighted the importance of aligning aeration strategies with lamp type and reactor design.

From a practical perspective, the findings of this study provide several useful insights for the design and operation of UV-based advanced oxidation processes. First, the strong correlation between oxidant decay and micropollutant degradation suggests that oxidant decay measurements can be used as a simple and cost-effective tool to evaluate and optimize reactor performance. This approach can reduce the need for extensive micropollutant analysis during early-stage testing and system optimization. The results indicate that microbubble aeration offers the greatest benefit when UV reactors operate under photon-limited conditions, such as at moderate oxidant doses or in systems prone to significant wall losses. Rather than increasing oxidant concentration or lamp power, controlled microbubble integration provides a passive method to improve photon utilization, which can help reduce chemical consumption and improve energy efficiency.

Overall, this study demonstrates that microbubble aeration is not simply a mixing enhancement, but an effective photon-management strategy that can significantly improve UV-AOP performance when applied within appropriate operating conditions. By linking oxidant decay, photon behavior, and treatment outcomes, the findings provide a practical and scalable framework for improving the efficiency of advanced water treatment systems.

3.7 Recommendations and Future Work

3.7.1 Recommendations

Based on the findings of this research, several recommendations are proposed to improve the performance, design, and practical implementation of microbubble-assisted UV-based Advanced Oxidation Processes (AOPs). These recommendations address both laboratory-scale optimization and considerations for full-scale water treatment applications.

The results of this study revealed that microbubble aeration improves photon utilization only within a specific range of bubble concentrations. Excessive bubbles reduce UV penetration due to excessive light shielding, whereas insufficient bubbles provide limited scattering benefits. Therefore, it is recommended that UV-AOP systems incorporate mechanisms to maintain optimal bubble density, either through adjustable aeration controls, variable-speed pumps, or flowrate-based modulation. Since flowrate demonstrated a strong influence on bubble concentration, it may be used effectively as an indirect control parameter in continuous-flow reactors.

A strong correlation was observed between the enhancement of oxidant decay ($k_{air}/k_{no\text{-}air}$) and micropollutant degradation. This demonstrates that oxidant-decay tests are a reliable and cost-effective surrogate for predicting micropollutant removal performance. Thus, it is recommended that future experimental studies and treatment facilities adopt oxidant decay measurements as a rapid pre-screening method for selecting optimal reactor configurations, oxidant doses, aeration rates, and lamp types. This study found that high concentrations of H_2O_2 or free chlorine diminished the enhancement effect of microbubble aeration due to increased radical scavenging and reduced photon limitation. Therefore, oxidant doses should be maintained at moderate levels to maximize the benefits of microbubble-induced photon

scattering and reflection. This has direct implications for cost optimization and operational efficiency. Medium-pressure (MP) UV lamps showed a more pronounced benefit from aeration than low-pressure (LP) lamps due to their broader spectral emission and inherently higher photon losses. Consequently, MP UV systems should be prioritized in applications where contaminant removal efficiency, photon utilization, or treatment of highly resistant micropollutants is critical. The enhanced effect of microbubbles can reduce energy consumption by improving overall UV utilization, potentially lowering the number of lamps required.

While this study demonstrates the technical benefits of microbubble aeration, the economic implications of introducing bubbles into UV-AOP systems must also be considered. Aeration requires additional energy input to operate pumps and diffusers, and the cost may vary depending on reactor size, bubble generation method, and operational flowrate. In small UV reactors, the energy demand for generating microbubbles is expected to be relatively low. However, in larger treatment systems, the cost of continuous aeration could become more significant if not optimized. Therefore, future studies should include a techno-economic assessment comparing the added energy cost of aeration with the potential savings from increased treatment efficiency, reduced oxidant consumption, and extended lamp life. Such analysis will help determine whether the net impact of microbubble integration is economically favorable for full-scale implementation.

Microbubbles provided secondary benefits, including reduced fouling on reactor walls, enhanced turbulence, and suppression of scaling on quartz sleeves. These advantages contribute to improved reactor longevity and reduced maintenance frequency. For full-scale treatment systems, microbubble aeration may serve as a cleaner alternative to reflective coatings, which suffer from long-term degradation and fouling. Incorporating microbubbles is

therefore recommended not only for improved oxidation performance but also for extended operational reliability.

3.7.2 Future Work

Investigation of Microbubble and Nanobubble Size Effects

This study focused on microbubbles with an average diameter of approximately 80 μm. Nanobubbles (<1 μm) possess distinct physicochemical properties such as long residence times, high internal pressure, and unique refractive characteristics. Future studies should evaluate:

- nanobubble-only systems,
- mixed micro-/nano-bubble systems, and
- the effect of bubble size distribution on photon scattering efficiency.

These investigations may reveal synergistic benefits for radical formation and contaminant degradation.

Evaluation of Real Water Matrices

All experiments were conducted using tap water with relatively low turbidity and organic content. The performance of microbubble-assisted UV-AOPs must be assessed under realistic conditions, including:

- Surface water
- Gound water
- Secondary wastewater effluent

- Industrial effluent containing dyes, NOM

Complex matrices may introduce additional radical scavengers, UV-absorbing substances, and interactions that influence bubble stability and photon transport.

Development of Optical Models for Photon–Bubble Interactions

While experimental observations confirmed that microbubbles extend photon path length through scattering and reflection, quantitative modeling was beyond the scope of this research. Future work should develop detailed optical models using:

- Monte Carlo photon transport simulations
- Radiative transfer equation (RTE) modeling
- Bubble scattering phase-function analysis

Such modeling will allow predictive optimization of bubble size, bubble density, reactor geometry, and lamp placement, enabling more efficient reactor designs.

Pilot-Scale and Full-Scale Validation

Scaling the microbubble-enhanced UV-AOP system requires consideration of hydrodynamics, bubble residence time, energy consumption, and photon distribution. Future work should include:

- Pilot-scale studies (hundreds to thousands of liters)
- Computational fluid dynamics (CFD) simulations of bubble trajectories and UV fields
- Energy-efficiency analysis

- Evaluation of lamp reduction potential

These efforts are essential to transition the technology from laboratory experimentation to practical water treatment applications.

REFERENCES

Ahmed, A. K. A., Sun, C., Hua, L., Zhang, Z., Zhang, Y., Zhang, W., & Marhaba, T. (2018). Generation of nanobubbles by ceramic membrane filters: The dependence of bubble size and zeta potential on surface coating, pore size and injected gas pressure. Chemosphere, 203, 327–335. https://doi.org/10.1016/j.chemosphere.2018.03.157

Abanyie, S. K., Apea, O. B., Abagale, S. A., Amuah, E. E. Y., & Sunkari, E. D. (2023). Sources and factors influencing groundwater quality and associated health implications: A review. Emerging Contaminants, 9(2), 100207. https://doi.org/10.1016/j.emcon.2023.100207

Abdel-Fatah, M. A. (2018). Nanofiltration systems and applications in wastewater treatment: Review article. Ain Shams Engineering Journal, 9(4), 3077–3092. https://doi.org/10.1016/j.asej.2018.08.001

Agarwal, A., Ng, W.J. and Liu, Y. (2011) Principle and applications of microbubble and nanobubble technology for water treatment. Chemosphere, 84, 1175–1180. https://doi.org/10.1016/j.chemosphere.2011.05.054

Al-Nuaim, M. A., Alwasiti, A. A., & Shnain, Z. Y. (2022). The photocatalytic process in the treatment of polluted water. Chemical Papers, 77(2), 677–701. https://doi.org/10.1007/s11696-022-02468-7

Ameta, R., & Ameta, S. (2018). Advanced oxidation processes for wastewater treatment: Emerging green chemical technology. In Advanced Oxidation Processes for Wastewater Treatment: Emerging Green Chemical Technology.

Ankit, Saha, L., Kumar, V., Tiwari, J., Sweta, Rawat, S., Singh, J., & Bauddh, K. (2021). Electronic waste and their leachates impact on human health and environment: Global ecological threat and management. Environmental Technology & Innovation, 24, 102049. https://doi.org/10.1016/j.eti.2021.102049

Anyame Bawa, S., Chan, A., Wrobel-Tobiszewska, A., Hardie, M., & Towns, C. (2024). A review of methods for mitigating microplastic contamination in biosolids from wastewater treatment plants before agricultural soil application. Science of The Total Environment, 957, 177360. https://doi.org/10.1016/j.scitotenv.2024.177360

Autin, O., Romelot, C., Rust, L., Hart, J., Jarvis, P., MacAdam, J., Parsons, S. A., & Jefferson, B. (2013). Evaluation of a UV-light emitting diodes unit for the removal of micropollutants in water for low energy advanced oxidation processes. Chemosphere, 92(6), 745–751. https://doi.org/10.1016/j.chemosphere.2013.04.028

Awawdeh, M., Al-Rousan, Z., & Alkaraki, K. (2023). Wastewater treatment plant site selection using GIS and multicriteria decision analysis. Arab Gulf Journal of Scientific Research, 42(4), 1504–1517. https://doi.org/10.1108/agjsr-09-2023-0412

Azevedo, A., Etchepare, R., Calgaroto, S., & Rubio, J. (2016). Aqueous dispersions of nanobubbles: Generation, properties and features. Minerals Engineering, 94, 29–37. https://doi.org/10.1016/j.mineng.2016.05.001

Baylar, A., & Ozkan, F. (2006). Applications of venturi principle to water aeration systems. Environmental Fluid Mechanics, 6(4), 341–357. https://doi.org/10.1007/s10652-005-5664-9

Belete, B., Desye, B., Ambelu, A., & Yenew, C. (2023). Micropollutant removal efficiency of advanced wastewater treatment plants: A systematic review. Environmental Health Insights, 17. https://doi.org/10.1177/11786302231195158

Bhattacharjee, S. (2016). DLS and zeta potential - What they are and what they are not? Journal of Controlled Release, 235, 337–351. https://doi.org/10.1016/j.jconrel.2016.06.017

Bittelli, M., Pellegrini, S., Olmi, R., Andrenelli, M. C., Simonetti, G., Borrelli, E., & Morari, F. (2022). Experimental evidence of laser diffraction accuracy for particle size analysis. Geoderma, 409, 115627. https://doi.org/https://doi.org/10.1016/j.geoderma.2021.115627

Bolton, J. R., & Stefan, M. I. (2002). Fundamental photochemical approach to the concepts of fluence (UV dose) and electrical energy efficiency in photochemical degradation reactions. Research on Chemical Intermediates, 28(7–9), 857–870. https://doi.org/10.1163/15685670260469474

Buxton, G.V. et al. (1988). Critical Review of Rate Constants for Reactions of Hydrated Electrons, H and OH Radicals in Aqueous Solution. J. Phys. Chem. Ref. Data. (~10⁹ compilation)

Calgaroto, S., Azevedo, A., Rubio, J., 2015. Flotation of quartz particles assisted by nanobubbles. Int. J. Miner. Process. 137, 64–70. https://doi.org/10.1016/j. minpro.2015.02.010.

Cantwell, R. E., & Hofmann, R. (2011). Ultraviolet absorption properties of suspended particulate matter in untreated surface waters. Water Research, 45(3), 1322–1328. https://doi.org/10.1016/j.watres.2010.10.020

Carpenter, D. O. (2006). Polychlorinated biphenyls (PCBs): routes of exposure and effects on human health. Reviews on Environmental Health, 21(1), 1-23.

Castro-Jiménez, C. C., Grueso-Domínguez, M. C., Correa-Ochoa, M. A., Saldarriaga-Molina, J. C., & García, E. F. (2022). A coagulation process combined with a multi-stage filtration system for drinking water treatment: An alternative for small communities. Water, 14(20), 3256. https://doi.org/10.3390/w14203256

Cesaro, A., & Belgiorno, V. (2016). Removal of endocrine disruptors from urban wastewater by advanced oxidation processes (aops): A review. The Open Biotechnology Journal, 10(1), 151–172. https://doi.org/10.2174/1874070701610010151

Chae, S. H., Kim, M. S., Kim, J.-H., & Fortner, J. D. (2023). Nanobubble Reactivity: Evaluating Hydroxyl Radical Generation (or Lack Thereof) under Ambient Conditions. ACS ES&T Engineering, 3(10), 1504–1510. https://doi.org/10.1021/acsestengg.3c00124

Chen, T., Wang, C., Andrews, S., & Hofmann, R. (2021). Effects of UV light path length and wavelength on uv/chlorine versus UV/H2O2 efficacy. ACS ES&T Water, 1(5), 1145–1152. https://doi.org/10.1021/acsestwater.0c00175

Cizmas, L., Sharma, V. K., Gray, C. M., & McDonald, T. J. (2015). Pharmaceuticals and personal care products in waters: Occurrence, toxicity, and risk. Environmental Chemistry Letters, 13(4), 381–394. https://doi.org/10.1007/s10311-015-0524-4

Couto, H., Nunes, D. G., Neumann, R., & França, S. (2009, March 1). Micro-bubble size distribution measurements by laser diffraction technique. Elsevier BV. https://www.researchgate.net/publication/248476089_Micro-bubble_size_distribution_measurements_by_laser_diffraction_technique

Cuerda-Correa, E. M., Alexandre-Franco, M. F., & Fernández-González, C. (2020). Advanced Oxidation Processes for the Removal of Antibiotics from Water. An Overview. Water, 12(1), 102. https://doi.org/10.3390/w12010102

Dar, M. A., Palsania, P., Satya, S., Dashora, M., Bhat, O. A., Parveen, S., Patidar, S. K., & Kaushik, G. (2025). Microplastic pollution: A global perspective in surface waters, microbial degradation, and corresponding mechanism. Marine Pollution Bulletin, 210, 117344. https://doi.org/10.1016/j.marpolbul.2024.117344

El Hammoudani, Y., Dimane, F., Haboubi, K., Benaissa, C., Benaabidate, L., Bourjila, A., Achoukhi, I., El Boudammoussi, M., Faiz, H., Touzani, A., Moudou, M., & Esskifati, M. (2024). Micropollutants in wastewater treatment plants: A bibliometric - Bibliographic study. *Desalination and Water Treatment*, *317*, 100190. https://doi.org/10.1016/j.dwt.2024.100190

Etchepare, I., Oliveira, G., & Azuma, C. (2017). Microbubble and nanobubble-based gas flotation for oily wastewater treatment: A review. Environmental Reviews, 25(4), 413–430.

Fan, W., Li, Y., Wang, C., Duan, Y., Huo, Y., Januszewski, B., Sun, M., Huo, M., & Elimelech, M. (2021). Enhanced Photocatalytic Water Decontamination by Micro–Nano Bubbles: Measurements and Mechanisms. Environmental Science & Technology, 55(10), 7025–7033. https://doi.org/10.1021/acs.est.0c08787

Fang, J., Shang, C., & Zhang, T. (2014). Quantitative evaluation of chlorine radical reactivity toward aromatic pollutants using benzoic acid as a probe. Environmental Science & Technology, 48(17), 10104–10112. https://doi.org/10.1021/es502439a

Frew, J. E., Jones, P., & Scholes, G. (1983). Spectrophotometric determination of hydrogen peroxide and organic hydropheroxides at low concentrations in aqueous solution. Analytica Chimica Acta, 155, 139–150. https://doi.org/https://doi.org/10.1016/S0003-2670(00)85587-7

Gao, Y., Saedi, Z., Shi, H., Zeng, B., Zhang, B., & Zhang, X. (2024). Machine learning-assisted optimization of microbubble-enhanced cold plasma activation for water treatment. ACS ES&T Water, 4(2), 735–750. https://doi.org/10.1021/acsestwater.3c00783

Glaze, W. H., Kang, J.-W., & Chapin, D. H. (1987). The chemistry of water treatment processes involving ozone, hydrogen peroxide and ultraviolet radiation. Ozone: Science & Engineering, 9(4), 335–352. https://doi.org/10.1080/01919518708552148

Gopalakrishnan, G., Jeyakumar, R. B., & Somanathan, A. (2023). Challenges and emerging trends in advanced oxidation technologies and integration of advanced oxidation processes with biological processes for wastewater treatment. Sustainability, 15(5), 4235. https://doi.org/10.3390/su15054235

Grandclément, C., Seyssiecq, I., Piram, P., Vimeux, F., & Moulis, C. (2017). From the conventional biological wastewater treatment to hybrid processes, the evaluation of organic micropollutant

removal: A review. Water Research, 111, 297–317. https://doi.org/10.1016/j.watres.2017.01.005

Grenni, P., Patrolecco, L., Rauseo, J., Spataro, F., Di Lenola, M., Aimola, G., Zacchini, M., Pietrini, F., Di Baccio, D., Stanton, I.C., Gaze, W.H., Barra Caracciolo, A., 2019. Sulfamethoxazole persistence in a river water ecosystem and its effects on the natural microbial community and Lemna minor plant. Microchem. J, Dev. Appl. Microtechniques in All Branches Sci. 149 (103999). https://doi.org/10.1016/j

Gupta, S.K., Rachna, Singh, B., Mungray, A.K., Bharti, R., Nema, A.K., Pant, K.K., Mulla, S.I., 2022. Bioelectrochemical technologies for removal of xenobiotics from wastewater. Sustain. Energy Technol. Assessments 49 (101652), 101652. https:// doi.org/10.1016/j.seta.2021.101652

Guerra-Rodríguez, S., Rodríguez, E., Singh, D., & Rodríguez-Chueca, J. (2018). Assessment of sulfate radical-based advanced oxidation processes for water and wastewater treatment: A review. Water, 10(12), 1828. https://doi.org/10.3390/w10121828

Han, T., Li, W., Li, J., Jia, L., Wang, H., & Qiang, Z. (2022). Degradation of micropollutants in flow-through UV/chlorine reactors: Kinetics, mechanism, energy requirement and toxicity evaluation. Chemosphere, 307, 135890. https://doi.org/10.1016/j.chemosphere.2022.135890

Heidarinejad, G., Bozorgmehr, N., & Safarzadeh, M. (2020). Effect of highly reflective material on the performance of water ultraviolet disinfection reactor. Journal of Water Process Engineering, 36, 101375. https://doi.org/10.1016/j.jwpe.2020.101375

Hoigné, J. (1998). Chemistry of Aqueous Ozone and Transformation of Pollutants by Ozonation in Water. In Handbook of Ozone Technology and Applications. (Definitive - OH review; rate constants, E⁰ table)

Hübner, U., Spahr, S., Lutze, H., Wieland, A., Rüting, S., Gernjak, W., & Wenk, J. (2024). Advanced oxidation processes for water and wastewater treatment - Guidance for systematic future research. Heliyon, 10(9), e30402. https://doi.org/10.1016/j.heliyon.2024.e30402

Hu, C. (2021). Reactor design and selection for effective continuous manufacturing of pharmaceuticals. Journal of Flow Chemistry, 11(3), 243–263. https://doi.org/10.1007/s41981-021-00164-3

Ijpelaar, G. F., Harmsen, D. J. H., Beerendonk, E. F., van Leerdam, R. C., Metz, D. H., Knol, A. H., Fulmer, A., & Krijnen, S. (2010). Comparison of low pressure and medium pressure UV lamps for uv/h2o2treatment of natural waters containing micro pollutants. Ozone: Science & Engineering, 32(5), 329–337. https://doi.org/10.1080/01919512.2010.508017

Innocenzi, V., Mazziotti di Celso, G., & Prisciandaro, M. (2020). Techno-economic analysis of olive wastewater treatment with a closed water approach by integrated membrane processes and advanced oxidation processes. Journal of Water Reuse and Desalination, 11(1), 122–135. https://doi.org/10.2166/wrd.2020.066

Jaimes-López, R., Jiménez-Vázquez, A., Pérez-Rodríguez, S., Estudillo-Wong, L. A., & Alonso-Vante, N. (2024). Catalyst for the generation of OH radicals in advanced electrochemical oxidation processes: Present and future perspectives. Catalysts, 14(10), 703. https://doi.org/10.3390/catal14100703

Jiang, T., Wu, W., Ma, M., Hu, Y., & Li, R. (2024). Occurrence and distribution of emerging contaminants in wastewater treatment plants: A globally review over the past two decades. Science of The Total Environment, 951, 175664. https://doi.org/10.1016/j.scitotenv.2024.175664

John, A., Brookes, A., Carra, I., Jefferson, B., & Jarvis, P. (2020). Microbubbles and their application to ozonation in water treatment: A critical review exploring their benefit and future application. Critical Reviews in Environmental Science and Technology, 52(9), 1561–1603. https://doi.org/10.1080/10643389.2020.1860406

Kaur, R., Talan, A., Tiwari, B., Pilli, S., Sellamuthu, B., & Tyagi, R. D. (2020). Constructed wetlands for the removal of organic micro-pollutants. In Current Developments in Biotechnology and Bioengineering (pp. 87–140). Elsevier. https://doi.org/10.1016/b978-0-12-819594-9.00005-x

Kayode-Afolayan, S. D., Ahuekwe, E. F., & Nwinyi, O. C. (2022). Impacts of pharmaceutical effluents on aquatic ecosystems. Scientific African, 17, e01288. https://doi.org/10.1016/j.sciaf.2022.e01288

Khader, E. H., Muslim, S. A., Saady, N. M. C., Ali, N. S., Salih, I. K., Mohammed, T. J., Albayati, T. M., & Zendehboudi, S. (2024). Recent advances in photocatalytic advanced oxidation processes for organic compound degradation: A review. Desalination and Water Treatment, 318, 100384. https://doi.org/10.1016/j.dwt.2024.100384

Khajouei, G., Finklea, H. O., & Lin, L.-S. (2022). UV/chlorine advanced oxidation processes for degradation of contaminants in water and wastewater: A comprehensive review. Journal of Environmental Chemical Engineering, 10(3), 107508. https://doi.org/10.1016/j.jece.2022.107508

Kizhisseri, M. I., Sakr, M., Maraqa, M., & Mohamed, M. M. (2025). A comparative bench scale study of oxygen transfer dynamics using micro-nano bubbles and conventional aeration in water treatment systems. Heliyon, 11(4), e41687. https://doi.org/10.1016/j.heliyon.2025.e41687

K'oreje, K.O., Kandie, F.J., Vergeynst, L., Abira, M.A., Van Langenhove, H., Okoth, M., Demeestere, K., 2018. Occurrence, fate and removal of pharmaceuticals, personal care products and pesticides in wastewater stabilization ponds and receiving rivers in the Nzoia Basin, Kenya. Sci. Total Environ. 637–638, 336–348. https://doi.org/ 10.1016/j.scitotenv.2018.04.331

Kucuk, E., Pilevneli, T., Onder Erguven, G., Aslan, S., Olgun, E.¨O., Canlı, O., Unlu, K., Dilek, F.B., Ipek, U., Avaz, G., Yetis, U., 2021. Occurrence of micropollutants in the yesilirmak river basin, Turkey. Environ. Sci. Pollut. Res. Int. 28 (19), 24830–24846. https://doi.org/10.1007/s11356-021-13013-6

Kukizaki, M., & Baba, Y. (2008). Effect of surfactant type on microbubble formation behavior using Shirasu porous glass (SPG) membranes. Colloids and Surfaces A: Physicochemical and Engineering Aspects, 326(3), 129–137. https://doi.org/10.1016/j.colsurfa.2008.05.025

Kumar, V., Sharma, N., Sharma, P., Pasrija, R., Kaur, K., Umesh, M., & Thazeem, B. (2023). Toxicity analysis of endocrine disrupting pesticides on non-target organisms: A critical analysis on toxicity mechanisms. *Toxicology and Applied Pharmacology*, *474*, 116623. https://doi.org/10.1016/j.taap.2023.116623

Kumari, P., & Kumar, A. (2023). ADVANCED OXIDATION PROCESS: A remediation technique for organic and non-biodegradable pollutant. Results in Surfaces and Interfaces, 11, 100122. https://doi.org/10.1016/j.rsurfi.2023.100122

Lagunas-Solar, M. (2014). Food Technologies: Pulsed Ultraviolet Radiation Processing. Encyclopedia of Food Safety. Elsevier.

Lauria, B. J., & Company, M. I. (2019). Venturi Injectors. January, 26–28.

Lee, C. H., Choi, H., Jerng, D.-W., Kim, D. E., Wongwises, S., & Ahn, H. S. (2019). Experimental investigation of microbubble generation in the venturi nozzle. International Journal of Heat and Mass Transfer, 136, 1127–1138. https://doi.org/10.1016/j.ijheatmasstransfer.2019.03.040

Li, H., Hu, L., & Xia, Z. (2013). Impact of Groundwater Salinity on Bioremediation Enhanced by Micro-Nano Bubbles. Materials, 6(9), 3676–3687.

Li, W., Li, M., Bolton, J. R., Qu, J., & Qiang, Z. (2017). Impact of inner-wall reflection on UV reactor performance as evaluated by using computational fluid dynamics: The role of diffuse reflection. Water Research, 109, 382–388. https://doi.org/10.1016/j.watres.2016.11.068

Lin, L., Yang, H., & Xu, X. (2022). Effects of water pollution on human health and disease heterogeneity: A review. *Frontiers in Environmental Science*, *10*. https://doi.org/10.3389/fenvs.2022.880246

Liu, Z., Hosseinzadeh, S., Wardenier, N., Verheust, Y., Chys, M., & Hulle, S. V. (2018). Combining ozone with UV and H2O2 for the degradation of micropollutants from different origins: Lab-scale analysis and optimization. Environmental Technology, 40(28), 3773–3782. https://doi.org/10.1080/09593330.2018.1491630

Liu, Z., Xu, B., Zhang, T.-Y., Hu, C.-Y., Tang, Y.-L., Dong, Z.-Y., Cao, T.-C., & El-Din, M. G. (2021). Formation of disinfection by-products in a UV-activated mixed chlorine/chloramine system. Journal of Hazardous Materials, 407, 124373. https://doi.org/10.1016/j.jhazmat.2020.124373

Luo, Y., Guo, W., Ngo, H. H., Nghiem, L. D., Hai, F. I., Zhang, J., Liang, S., & Wang, X. C. (2014). A review on the occurrence of micropollutants in the aquatic environment and their fate and removal during wastewater treatment. The Science of the Total Environment, 473–474, 619–641. https://doi.org/10.1016/j.scitotenv.2013.12.065

Mackey, E., Hofmann, R., Festger, A., Vanyo, C., Moore, N., Chen, T., Wang, C., Taylor-Edmonds, L., & Andrews, S. A. (2023). UV-chlorine advanced oxidation for potable water reuse: A review of the current state of the art and research needs. Water Research X, 19, 100183. https://doi.org/https://doi.org/10.1016/j.wroa.2023.100183

Marlatt, V. L., Bayen, S., Castaneda-Cortès, D., Delbès, G., Grigorova, P., Langlois, V. S., Martyniuk, C. J., Metcalfe, C. D., Parent, L., Rwigemera, A., Thomson, P., & Van Der Kraak, G. (2022). Impacts of endocrine disrupting chemicals on reproduction in wildlife and humans. Environmental Research, 208, 112584. https://doi.org/10.1016/j.envres.2021.112584

Martín-Sómer, M., Moreira, J., Santos, C., Gomes, A. I., Moreno-SanSegundo, J., Vilar, V. J. P., & Marugán, J. (2023). Reflector design for the optimization of photoactivated processes in tubular reactors for water treatment. Journal of Environmental Chemical Engineering, 11(5), 110609. https://doi.org/10.1016/j.jece.2023.110609

Martinez, J. L. (2009). Environmental pollution by antibiotics and by antibiotic resistance determinants. Environmental Pollution, 157(11), 2893–2902. https://doi.org/10.1016/j.envpol.2009.05.051

Mbonimpa, E. G., Vadheim, B., & Blatchley, E. R., III. (2012). Continuous-flow solar UVB disinfection reactor for drinking water. Water Research, 46(7), 2344–2354. https://doi.org/10.1016/j.watres.2012.02.003

Mei, J., Gao, X., Zou, J., & Pang, F. (2023). Research on photocatalytic wastewater treatment reactors: Design, optimization, and evaluation criteria. Catalysts, 13(6), 974. https://doi.org/10.3390/catal13060974Chae, S. H., Kim, M. S., Kim, J.-H., & Fortner, J. D. (2023). Nanobubble Reactivity: Evaluating Hydroxyl Radical Generation (or Lack Thereof) under Ambient Conditions. ACS ES&T Engineering, 3(10), 1504–1510. https://doi.org/10.1021/acsestengg.3c00124

Meng, T., Su, X., Sun, P., Sun, W., Santoro, D., Yao, H., & Wang, H. (2023). UV-based advanced oxidation processes in photoreactors with reflective sleeves. Journal of Cleaner Production, 416, 137945. https://doi.org/https://doi.org/10.1016/j.jclepro.2023.137945

Miklos, D. B., Wang, W.-L., Linden, K. G., Drewes, J. E., & Hübner, U. (2018). Comparison of UV-AOPs (UV/H2O2, UV/PDS and UV/Chlorine) for TOrC removal from municipal wastewater effluent and optical surrogate model evaluation. Chemical Engineering Journal, 362, 537–547. https://doi.org/10.1016/j.cej.2019.01.041

Miletta, B. A., Amano, R. S., Alkhalidi, A. A. T., & Li, J. (2011). Study of air bubble formation for wastewater treatment. Volume 2: 31st Computers and Information in Engineering Conference, Parts A and B, 275–280. https://doi.org/10.1115/detc2011-47065

Mustafa, S. A., Al-Rudainy, A. J., & Salman, N. M. (2024). Effect of environmental pollutants on fish health: An overview. Egyptian Journal of Aquatic Research, 50(2), 225–233. https://doi.org/10.1016/j.ejar.2024.02.006

Mwanga, N., Wang, X., Li, P., Liu, Y., Xia, S., Yin, D., Rui, M., & Ye, Y. (2024). Effect of micro and nanobubble size and concentration on membrane fouling: Strategies for energy-saving and ultrafiltration efficiency enhancement. Desalination, 587, 117929. https://doi.org/https://doi.org/10.1016/j.desal.2024.117929

Nimma, D., Devi, O. R., Laishram, B., Ramesh, J. V. N., Boddupalli, S., Ayyasamy, R., Tirth, V., & Arabil, A. (2025). Implications of climate change on freshwater ecosystems and their biodiversity. Desalination and Water Treatment, 321, 100889. https://doi.org/10.1016/j.dwt.2024.100889

Ning, R., Yu, S., Li, L., Snyder, S. A., Li, P., Liu, Y., Togbah, C. F., & Gao, N. (2024). Micro and nanobubbles-assisted advanced oxidation processes for water decontamination: The importance of interface reactions. Water Research, 265, 122295. https://doi.org/https://doi.org/10.1016/j.watres.2024.122295

Ning, R., Snyder, S. A., Ma, J., Wang, D., Li, P., Xiao, Q., Xiang, Y., Fan, G., Yan, Z., Gao, N., Yu, S., & Li, L. (2025). Interface Effects of Micro/nanobubbles Enable Selective Photooxidation of Contaminants. Environmental Science & Technology. https://doi.org/10.1021/acs.est.5c11061

Nishmitha, P. S., Akhilghosh, K. A., Aiswriya, V. P., Ramesh, A., Muthuchamy, M., & Muthukumar, A. (2025). Understanding emerging contaminants in water and wastewater: A comprehensive review on detection, impacts, and solutions. Journal of Hazardous Materials Advances, 18, 100755. https://doi.org/10.1016/j.hazadv.2025.100755

Parnis, J. M., & Oldham, K. B. (2013). Beyond the Beer–Lambert law: The dependence of absorbance on time in photochemistry. Journal of Photochemistry and Photobiology A: Chemistry, 267, 6–10. https://doi.org/10.1016/j.jphotochem.2013.06.006

Patel, S. K., Shukla, S. C., Natarajan, B. R., Asaithambi, P., Dwivedi, H. K., Sharma, A., Singh, D., Nasim, M., Raghuvanshi, S., Sharma, D., Sen, S., Dubey, S., & Prajapati, A. K. (2025). State of the art review for industrial wastewater treatment by electrocoagulation process: Mechanism, cost and sludge analysis. Desalination and Water Treatment, 321, 100915. https://doi.org/10.1016/j.dwt.2024.100915

Pavi, C. P., Elois, M. A., Jempierre, Y. F. S. H., Cadamuro, R. D., Savi, B. P., Pilati, G. V. T., & Fongaro, G. (2025). Micropollutants and their interactions with relevant environmental viruses. Environmental Microbiology, 27(10). https://doi.org/10.1111/1462-2920.70184

Pera-Titus, M., García-Molina, V., Baños, M. A., Giménez, J., & Esplugas, S. (2004). Degradation of chlorophenols by means of advanced oxidation processes: A general review. Applied Catalysis B: Environmental, 47(4), 219–256. https://doi.org/10.1016/j.apcatb.2003.09.010

Petrie, B., Barden, R., & Kasprzyk-Hordern, B. (2015). A review on emerging contaminants in wastewaters and the environment: Current knowledge, understudied areas and recommendations for future monitoring. *Water Research*, *72*, 3–27. https://doi.org/10.1016/j.watres.2014.08.053

Postigo, C., Gil-Solsona, R., Herrera-Batista, M.F., Gago-Ferrero, P., Alygizakis, N., Ahrens, L., Wiberg, K., 2021. A step forward in the detection of byproducts of anthropogenic organic micropollutants in chlorinated water. Trends Environ. Anal. Chem. 32 (e00148), e00148. https://doi.org/10.1016/j.teac.2021.e00148.

Pignatello, J.J. et al. (2006). Advanced Oxidation Processes for Organic Contaminant Destruction Based on the Fenton Reaction. Crit. Rev. Environ. Sci. Technol. (Non-corrosive, economic)

Pradhan, B., Chand, S., Chand, S., Rout, P. R., & Naik, S. K. (2023). Emerging groundwater contaminants: A comprehensive review on their health hazards and remediation technologies. Groundwater for Sustainable Development, 20, 100868. https://doi.org/10.1016/j.gsd.2022.100868

Pulicharla, R., Proulx, F., Behmel, S., Sérodes, J.-B., & Rodriguez, M. J. (2020). Trends in ozonation disinfection by-products—occurrence, analysis and toxicity of carboxylic acids. Water, 12(3), 756. https://doi.org/10.3390/w12030756

Ran, J., Liu, J., Zhang, C., Wang, D., & Li, X. (2013). Experimental investigation and modeling of flotation column for treatment of oily wastewater. International Journal of Mining Science and Technology, 23(5), 665–668. https://doi.org/https://doi.org/10.1016/j.ijmst.2013.08.008

Rekhate, C. V., & Srivastava, J. K. (2020). Recent advances in ozone-based advanced oxidation processes for treatment of wastewater- A review. Chemical Engineering Journal Advances, 3, 100031. https://doi.org/10.1016/j.ceja.2020.100031

Richardson, S. D., Plewa, M. J., Wagner, E. D., Schoeny, R., & DeMarini, D. M. (2007). Occurrence, genotoxicity, and carcinogenicity of regulated and emerging disinfection by-products in drinking water: A review and roadmap for research. Mutation Research/Reviews in Mutation Research, 636(1–3), 178–242. https://doi.org/10.1016/j.mrrev.2007.09.001

Rogowska, J., Cieszynska-Semenowicz, M., Ratajczyk, W., & Wolska, L. (2019). Micropollutants in treated wastewater. Ambio, 49(2), 487–503. https://doi.org/10.1007/s13280-019-01219-5

Romantschuk, M., Lahti-Leikas, K., Kontro, M., Galitskaya, P., Talvenmäki, H., Simpanen, S., Allen, J. A., & Sinkkonen, A. (2023). Bioremediation of contaminated soil and groundwater by in situ biostimulation. Frontiers in Microbiology, 14. https://doi.org/10.3389/fmicb.2023.1258148

Samal, K., Mahapatra, S., & Hibzur Ali, M. (2022). Pharmaceutical wastewater as Emerging Contaminants (EC): Treatment technologies, impact on environment and human health. Energy Nexus, 6, 100076. https://doi.org/10.1016/j.nexus.2022.100076

Sillanpää, M., Ncibi, M. C., Pulkka, S., & Wallis, P. (2018). Emerging pollutants in wastewater: A review through the combination of graphene-based adsorption and electrochemical degradation. Journal of Environmental Management, 210, 275–292. https://doi.org/10.1016/j.jenvman.2018.01.015

Singh, B. J., Chakraborty, A., & Sehgal, R. (2023). A systematic review of industrial wastewater management: Evaluating challenges and enablers. Journal of Environmental Management, 348, 119230. https://doi.org/10.1016/j.jenvman.2023.119230

Sisay, E. J., Al-Tayawi, A. N., László, Z., & Kertész, S. (2023). Recent advances in organic fouling control and mitigation strategies in membrane separation processes: A review. Sustainability, 15(18), 13389. https://doi.org/10.3390/su151813389

Shannon, M. A., Bohn, P. W., Elimelech, M., Georgiadis, J. G., Mariñas, B. J., & Mayes, A. M. (2008). Science and technology for water purification in the coming decades. *Nature*, *452*(7185), 301–310. https://doi.org/10.1038/nature06599

Sharpless, C. M., & Linden, K. G. (2003). Experimental and Model Comparisons of Low- and Medium-Pressure Hg Lamps for the Direct and H2O2 Assisted UV Photodegradation of N-Nitrosodimethylamine in Simulated Drinking Water. Environmental Science & Technology, 37(9), 1933–1940. https://doi.org/10.1021/es025814p

Sgroi, M., Snyder, S. A., & Roccaro, P. (2021). Comparison of AOPs at pilot scale: Energy costs for micro-pollutants oxidation, disinfection by-products formation and pathogens inactivation. Chemosphere, 273, 128527. https://doi.org/10.1016/j.chemosphere.2020.128527

Stehle, S., & Schulz, R. (2015). Pesticide authorization in the EU—environment unprotected? Environmental Science and Pollution Research, 22(24), 19632–19647. https://doi.org/10.1007/s11356-015-5148-5

Sturm, M. T., Myers, E., Schober, D., Thege, C., Korzin, A., & Schuhen, K. (2022). Adaptable process design as a key for sustainability upgrades in wastewater treatment: Comparative study on the removal of micropollutants by advanced oxidation and granular activated carbon processing at a German municipal wastewater treatment plant. Sustainability, 14(18), 11605. https://doi.org/10.3390/su141811605

Sun, P., Lee, W.-N., Zhang, R., & Huang, C.-H. (2016). Degradation of DEET and Caffeine under UV/Chlorine and Simulated Sunlight/Chlorine Conditions. Environmental Science & Technology, 50(24), 13265–13273. https://doi.org/10.1021/acs.est.6b02287

Takahashi, M., Ishikawa, H., Asano, T., & Horibe, H. (2012). Effect of microbubbles on ozonized water for photoresist removal. The Journal of Physical Chemistry C, 116(23), 12578–12583. https://doi.org/10.1021/jp301746g

Varsha, M., Senthil Kumar, P., Senthil Rathi, B., 2022. A review on recent trends in the removal of emerging contaminants from aquatic environment using low-cost adsorbents. Chemosphere 287 (Pt 3), 132270. https://doi.org/10.1016/j. chemosphere.2021.132270

Verlicchi, P., & Ghirardini, A. (2019). Occurrence of micropollutants in wastewater and evaluation of their removal efficiency in treatment trains: The influence of the adopted sampling mode. Water, 11(6), 1152. https://doi.org/10.3390/w11061152

Vilanova, A., Dias, P., Lopes, T., & Mendes, A. (2024). The route for commercial photoelectrochemical water splitting: A review of large-area devices and key upscaling challenges. Chemical Society Reviews, 53(5), 2388–2434. https://doi.org/10.1039/d1cs01069g

von Gunten, U. (2003). Ozonation of drinking water: Part I. Oxidation kinetics and product formation. Water Research, 37(7), 1443–1467. https://doi.org/10.1016/S0043-1354(02)00457-8

Wang, C., Moore, N., Bircher, K., Andrews, S., & Hofmann, R. (2019). Full-scale comparison of UV/H2O2 and UV/Cl2 advanced oxidation: The degradation of micropollutant surrogates and the formation of disinfection byproducts. Water Research, 161, 448–458. https://doi.org/10.1016/j.watres.2019.06.033

Wang, L., Peng, B., & Li, J. (2015). Microbubble size distribution measurement in a DAF system. Industrial & Engineering Chemistry Research, 54(20), 5678–5685. https://doi.org/10.1021/acs.iecr.5b00109

Wang, P., Wang, Z., Wu, Z., & Mai, S. (2011). Fouling behaviours of two membranes in a submerged membrane bioreactor for municipal wastewater treatment. Journal of Membrane Science, 382(1–2), 60–69. https://doi.org/10.1016/j.memsci.2011.07.044

Zhao, D., & Yu, S. (2015). A review of recent advance in fouling mitigation of NF/RO membranes in water treatment: Pretreatment, membrane modification, and chemical cleaning. Desalination and Water Treatment, 55(4), 870–891. https://doi.org/10.1080/19443994.2014.928804

Zhou, S., Marcelino, K. R., Wongkiew, S., Sun, L., Guo, W., Khanal, S. K., & Lu, H. (2022). Untapped Potential: Applying Microbubble and Nanobubble Technology in Water and Wastewater Treatment and Ecological Restoration. *ACS ES&T Engineering*, *2*(9), 1558–1573. https://doi.org/10.1021/acsestengg.2c00117

Appendix

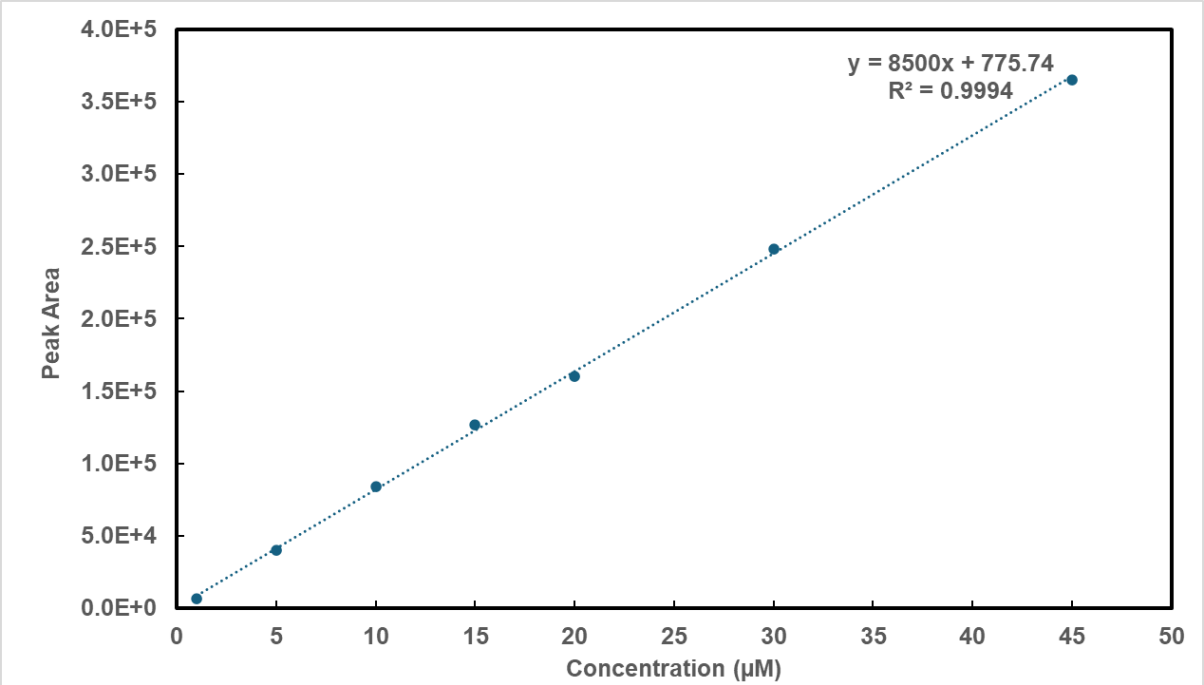

A1. Calibration curve for Caffeine

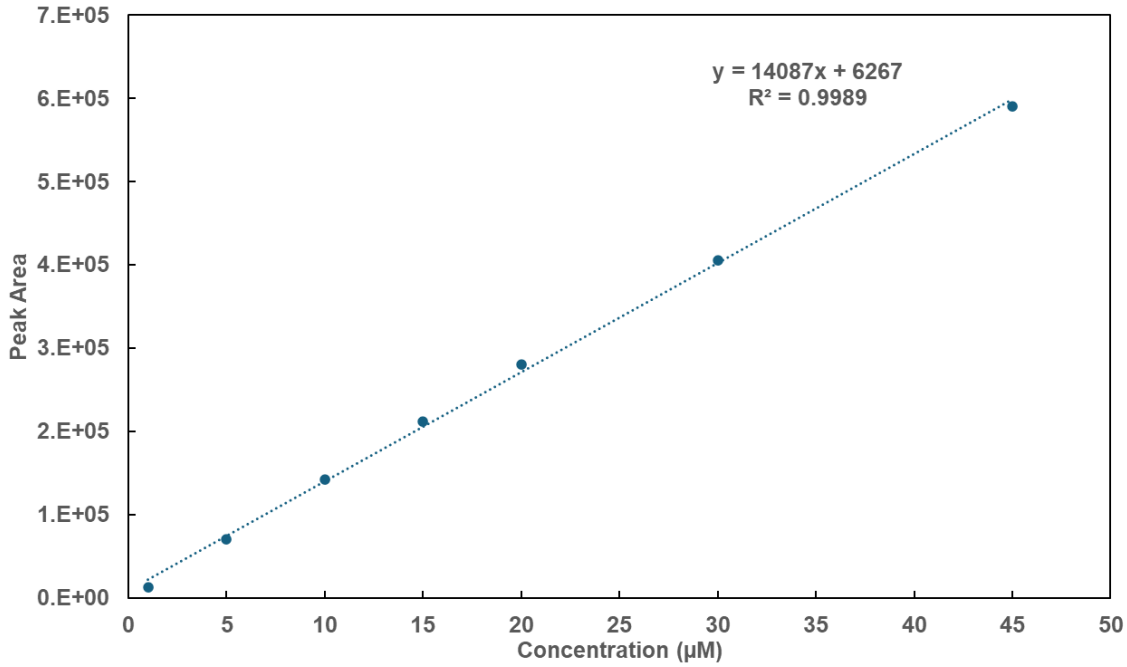

A2. Calibration curve for Benzoic Acid

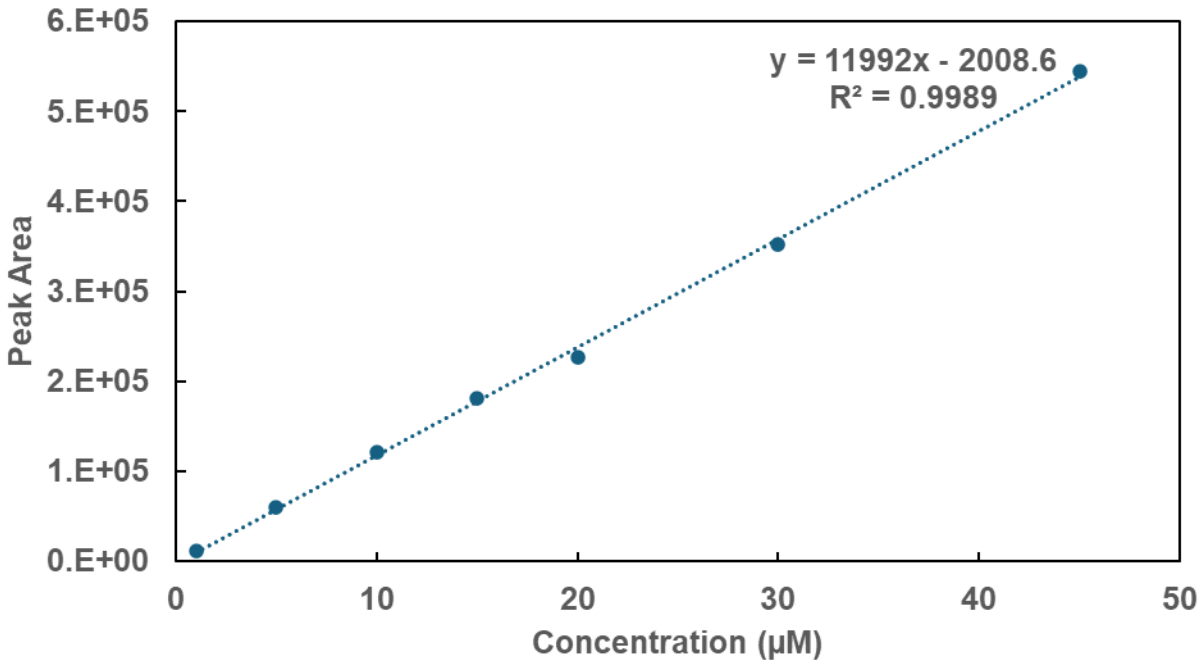

A3. Calibration curve for Nitrobenzene